Hydrocarbon Emissions in a Homogeneous Direct-Injection Spark Engine: Gasoline and Gasohol

by

Ronald Tharp

B.S. Mechanical Engineering
Massachusetts Institute of Technology, 2005

SUBMITTED TO THE DEPARTMENT OF MECHANICAL ENGINEERING IN PARTIAL FULFILLMENT OF THE REQUIREMENTS FOR THE DEGREE OF

MASTERS OF SCIENCE IN MECHANICAL ENGINEERING
AT THE
MASSACHUSETTS INSTITUTE OF TECHNOLOGY

June 2008

Signature of Author: _____
Department of Mechanical Engineering
May 9, 2008

Certified by: _____
Wai K. Cheng
Professor of Mechanical Engineering
Thesis Supervisor

Accepted by: _____
Lallit Anand
Chairman, Department Graduate Committee

Hydrocarbon Emissions in a Homogeneous Direct-Injection Spark Engine: Gasoline and Gasohol

by

Ronald Tharp

Submitted to the Department of Mechanical Engineering
On May 9, 2008 in Partial Fulfillment of the
Requirements for the Degree of Masters of Science in
Mechanical Engineering

Abstract

In order to better understand the effects on hydrocarbon emissions of loading, engine temperature, fuel type, and injection timing, a series of experiments was performed. The effect of loading was observed by running the engine at a higher temperature and more open throttle than would typically be observed at fast idle or low load driving. The effects of coolant temperature, the charge motion control valve, spark timing and rail pressure were tested through holding all other variables constant and sweeping through different injection timing to observe the effect on emissions and power output.

A new fuel system was designed to allow for the quick testing of different ethanol blends. The system allowed for comparison testing of an 85% ethanol blend to UTG 91 as a function of coolant temperature and injection timing. Measurement of cylinder pressure and hydrocarbon emissions near the exhaust valve allowed for a better understanding of engine operation and the effect of using high ethanol content fuels. Initial testing was also done on 15% and 40% ethanol blends.

The results revealed that engine emissions decrease as a function of reduced loading and higher engine temperatures. Sweeps of injection timings for all fuels demonstrated high hydrocarbon emissions for earlier injection timings which fell as injection timing was retarded. A secondary peak was observed in hydrocarbon emissions for an injection timing of approximately 150 CAD aTDC intake.

Analysis of rate of fuel injection vs. indicated power revealed a steady decrease in indicated efficiency as injection timing was retarded up to 120 CAD aTDC Intake and then a slow rise in efficiency as the timing was further retarded. The exact causes of the decrease in engine efficiency are unknown; however, possible explanations involve increased heat transfer from the cylinder and piston, fuel loss, and inefficient combustion due to impingement on cold surfaces.

Thesis Supervisor: Wai K. Cheng
Title: Professor of Mechanical Engineering

Acknowledgements

I would like to thank many people for their help in this project. First, I would like to thank the automotive and petroleum companies who are part of the Engine and Fuels consortium and support me in this research. I would like to especially thank the representatives of these companies who come to our consortiums, listen to my presentations, and then give me valuable advice and opinions based upon their significant knowledge and experience. A great amount of thanks also goes to my thesis advisor Wai Cheng who was kind enough to take me on and is always there to answer questions and listen to a hypothesis I have for the data. He also deserves a great amount of thanks for designing, maintaining, and modifying the engine control system for my engine without which my research would not be possible.

Additional acknowledgement must also be provided to the key support staff of the Sloan Automotive Lab. Thane DeWitt is always available to offer advice on what specifications are needed for parts, the best way to go about ordering them, and also how to solve the constant problems that occur when doing practical research. I and the entire Sloan Lab also owe a great deal of thanks to Raymond Phan whose skill and expertise as a technician and machinists have proved invaluable in making, fixing, and modifying components for my test cell.

I would also like to thank those members of the Sloan Automotive Lab who I have become friends with and have helped me countless times with my research. Steve Przesmitzki, Robert (RJ) Scaringe, Vince Costanzo, Dongkun Lee, Tairin Han, and Eric Senzer have always been there when I have a question about how to use a piece of equipment or for possible explanations for my data. For their assistance and friendship I owe them a large debt of gratitude.

Last but not least, I would like to thank my parents Steve and Margaret Tharp and my sister Kat. For my entire life they have always been there for me and supported me. It did not matter if it was a loan of money to pay for tuition after a bad month, late night phone calls when research or problem sets had me insane with worry, or just taking me out to dinner. My family is my rock and if I have accomplished anything, then it is because I have them to support me when I stumble.

Biographical Note

Ronald Tharp went to MIT for his undergraduate degree in mechanical engineering. His thesis focused on improvements to phosphoric acid fuel cell electrodes to improve electrical output as a function of volume, weight, and mass of catalyst used. As an undergraduate he was a leader in his fraternity and served in many offices. As a graduate student he has been an officer for graduate house and for the club rugby team he plays for. Between his undergraduate graduation and start of graduate school he worked for a local consulting company, BlazeTech, where he developed models for surface heating of projectiles and the potential for ignition of fuel vapors by means of hot-spot ignition. He has accepted an offer to do modeling and simulation work for Booz Allen Hamilton in Mclean, Virginia where he will work for their public sector division.

Nomenclature

aTDC / aBDC	after Top Dead Center / after Botton Dead Center
BDC	Bottom Dead Center
BMEP	Brake Mean Effective Pressure
BSFC	Brake Specific Fuel Consumption
bTDC / aTDC	before Top Dead Center / before Botton Dead Center
CAD	Crank Angle Degrees
CO	Carbon Monoxide
CO2	Carbn Dioxide
DI	Direct Injection
DISI	Direct Injection Spark Ignited
EOI	End of Injection
EVC	Exhaust Valve Closing
EVO	Exhaust Vale Opening
FFID	Fast Flame Ionization Detector
GDISI	Gasoline Direct Injection Spark Ignition
GIMEP	Gross Indicated Mean Effective Pressure
HC	Hyrocarbon
$\eta i,net$	Net Indicated Fuel Conversion Effeciency
ISFC	Indicated Specific Fuel Consumption
IMEP	Indicated Mean Effective Pressure
IVC	Intake Valve Closing
IVC	Intake Valve Opening
MAP	Manifold Absolute Pressure
MEP	Mean Effective Pressure
MPI	Multiport Fuel Injection
NIMEP	Net Indicated Mean Effective Pressure
NOx	Notrogen Oxides
PFI	Port Fuel Injection
PM	Particulate Matter
RTD	Resistance Temperature Detector
SMD	Sauter Mean Diameter
SOI	Start of Injection
TDC	Top Dead Center

Table of Contents

List of Figures

List of Tables

List of Appendices

1 Introduction

Currently the United States and world finds itself in an energy shortage if not an energy crisis. The increased industrialization of China, India, and other formerly third world countries has resulted in an explosive rise in the demand for oil. In the United States, the steadily increasing population, families having multiple cars and the growth of the SUV market have served to increase the already titanic demand for oil in the United States. The necessity to go to more remote locations, drill deeper to find oil deposits, and ship the oil farther has increased the energy required to mine oil and has thus reduced the net gain in oil per barrel removed from the ground. The combination of all these effects has recently resulted in the price of oil skyrocketing to over $100 per barrel with the associated rise of gasoline to almost $4 per gallon at the pumps.

Currently there is almost no buffer between the rate at which oil can be supplied and the rate at which it is demanded. As such, there is a growing concern that within the next decade the world will reach a peak oil production level and will be unable to match demand. The effect on the world economies and especially the United States which consumed a fourth of the world oil is hard to predict, but it would certainly have a profound impact on the mobility of the average American and result in a significant lifestyle change.

Another key issue in the world is the concept of emissions of smog producing gasses such as hydrocarbons (HC) and oxides of nitrogen (NO_x). Modern 3-way catalysts are quickly reaching 99% conversion efficiencies and have significantly reduced automotive emissions. However, these catalysts are only effective once they have reached their operating temperature, which requires several minutes using standard technology. A typical suburban drive cycle might be 15 minutes to the store, 30 minutes to shop during which the catalyst

cools down, and then a 15 minute trip back to the house. As such, for the majority of the time the catalyst is not working efficiently and it is critical that engine emissions be as low as possible during those times.

The mechanisms effecting hydrocarbon emissions in traditional port injection engines have been researched fairly extensively. As an example, a paper by Cheng et al. describes both the mechanisms contributing to hydrocarbon emissions and their relative effect [1]. It was found that crevices located in crevices around the spark plug, cylinder head gasket, piston and ring pack contributed approximately 38% of hydrocarbon emissions. The oil layers within the ring pack and on the cylinder walls were found to absorb hydrocarbons and then release these hydrocarbons into the exhaust following the combustion event, thus contributing about 16% of the total hydrocarbons. Deposits on the piston and cylinder contributed an additional 16% to hydrocarbon emissions by absorbing hydrocarbons within their porous structure and thus shielding them from combustion. Liquid fuel within the cylinder was found to add 20% of the total hydrocarbon emissions.

The duel problems of reducing fuel consumption and reducing emissions result in a difficult problem for car manufacturers and researchers. They must constantly strive to make their powertrains more efficient while also ensuring that the emissions during the first few minutes are as low as possible. The gasoline direct injection engine (GDI)[†] has several features that make it a viable solution for improving fuel economy in the near future such as charge cooling and the potential for higher compression ratios. However, it is critical that the level and type of emissions for this type of engine be analyzed and understood so as to reach a level of understand similar to that for port injection fuel system. This will serve to minimize the environmental impact of GDI engines and make this technology more appealing.

[†] The name, GDI, is a trademarked by Mitsubishi Motors Corporation. The term is used generically.

1.1 Background

Although GDI engines have only entered the mainstream within the past decade, they are by no means a new technology. Their potential for higher efficiency has resulted in several studies and strategies for implementing this technology.

1.1.1 Differences between the different forms of GDI technology

The basic concept of GDI is fairly simple. However, the ability to inject directly into the cylinder allows for increased flexibility which has spawned several different techniques.

1.1.1.1 Stratified Charges

A stratified charge system is used when the engine is running at part load. Rather than throttling the engine, the amount of air entering the cylinder is left unchanged and the power output is adjusted by varying the level of fuel. The net effect is that the fuel air mixture is lean overall. The combustion speed of a lean mixture is less than that of a stoichiometric or rich mixture. As such, if the mixture was homogenous if would burn too slowly and efficiency and engine performance would suffer. The piston cylinder incorporates special topography which directs the majority of the charge towards the spark plug. Injection is also done later to reduce the level of mixing that can occur. The overall effect is a stoichiometric or slightly rich mixture near the spark plug. This mixture burns quickly before the flame front moves into the lean portion of the mixture. By this point the lean mixture has become highly compressed and the flame front moves fast enough for the combustion event to finish in the required amount of time.

1.1.1.2 Homogenous Lean Charges

This technology is very similar to stratified charging. The piston does not provide any surface topography to create stratification and injection occurs early enough for mixing to occur and the resulting fuel air mixture is homogenous. Since the fuel mixture will burn slowly, this technique requires that either the engine be running at low speeds, which frequently occurs at low loads, or that a portion of the exhaust gasses be injected into the cylinder to increase the overall mixture temperature and increase the rate of combustion.

1.1.1.3 Homogenous Stoichiometric Charges

This is the closes analogy to PFI injection and is the type of system that is employed in our research. A throttle is used to control the amount of air that enters the cylinder. The amount of fuel injected corresponds to the amount of fuel needed to make a homogenous air-fuel mixture. The advantage of this system is that it allows the engine to use a three-way catalyst.

1.1.2 Efficiency

The primary motivation for the implementation of GDI engines is the potential for increased efficiency. In a standard PFI engine, the fuel is injected into the intake port outside of the fuel cylinder. Some of the fuel is vaporized immediately by the injection process interacting with the air flowing through the intake port. However, a large part is not vaporized and comes to land on the surface of the intake port, where a puddle is quickly formed. Initially the intake port is cold and little vaporization occurs and most fuel that enters the cylinder is through entanglement with the air and shearing off the top of the puddle. As such, more fuel needs to be injected than what is required to form a combustible charge, and

the puddle continues to grow. As the engine temperature rises, the walls of the intake port start to provide the heat to evaporate fuel in the puddle. Eventually equilibrium is reached in which the rate of fuel entanglement in the air, vaporization, and shearing off the top of the puddle is equal to the mass of fuel injected and the puddle stops growing.

In a GDI engine, the fuel is injected directly into the cylinder. This requires that higher pressure injectors be used in order to make smaller droplets than are seen in a port fuel injection system. The GDI design has several advantages over a PFI system. Since the fuel is injected directly into the cylinder, there is no need to produce a puddle and if designed correctly then all fuel that enters the cylinder undergoes combustion. As such, no extra fuel needs to be used during start-up.

Another advantage is a better transient response. In a PFI system, the size of the puddle always needs to be accounted for. The size of the puddle influences the amount of fuel that will be vaporized and the amount of fuel that will shear off the top of the puddle. As such, it is difficult to exactly determine the amount of fuel that needs to be injected when the level of throttling changes. This can result in the engine not running at its peak efficiency. This problem is exacerbated with frequent changes in throttling such as occur in city and suburban driving.

GDI engines also benefit from the charge cooling effect. When operating at full throttle, the mass of air inside the cylinder determines the maximum torque and horsepower of the engine. In a port fuel injection engine, the fuel is vaporized in the port and the temperature of the air in the port is approximately equal to the final temperature of the air in the cylinder when the intake valve closes. In a GDI engine, a large part of the heat to vaporize the fuel comes from the fuel charge. As such, the air inside the cylinder becomes colder and denser.

Since the air is denser, there is a larger mass of air in the cylinder and more torque and power can be produced from the same size engine.

Related to charge cooling is the advantage that can be observed in the area of knock prevention. Knock is the harmonic vibration of the engine cylinders that occurs when the air-fuel mixture away from the combustion front ignites via compression by the burned gasses which results in a very rapid rise in pressure. Depending on the level and intensity of knock, the effect can vary from an annoying pinging sound to severe damage to the piston, cylinder, and head. Knock occurs when the pressure and temperature in the cylinder becomes high enough for combustion to occur without an ignition source such as a spark or flame. PFI engines are limited to a compression ratio of around 10 because to operate at full load with a higher compression ratio results in knock or the spark timing having to be retarded from optimal to prevent knock. In a GDI engine, the previously mentioned vaporization of the injected fuel results in a lower charge temperature. This lower temperature means that for the same compression ratio and initial pressure, a GDI engine will have a lower charge temperature at the time of combustion. The result is that a GDI engine is less prone to knock than a PFI engine. As such, a GDI engine can be run at a higher compression ratio which results in a higher fuel conversion efficiency. This can be observed from Table 1-1 in which the fuel-air efficiency is estimated for different compression ratios.

All the previously mentioned efficiency benefits occur regardless of the type of GDI injection that is used. However, additional benefits can be observed if lean or stratified combustion is used. Since the focus of this research is homogenous stoichiometric GDI engines, these advantages are only briefly summarized below in Table 1-1 [2]

Specific heat ratio	Increased cycle efficiency due to incrementally higher specific heat ratio of lean mixtures
Heat Loss	Stratified Combustion results in lower temperatures near wall and lean combustion reduces overall heat loss
Pumping Loss	Unthrottled operation reduces pumping losses by not liming the flow of intake air which lowers the intake pressure

Table 1-1: Advantages of direct injection systems

Based upon the efficiency improvements, Andriesse et al. estimates an overall fuel economy benefit of 7 – 10% with a homogenous GDI system [3]. The largest benefit (3 – 4%) comes from charge cooling allowing the same power and torque to be produced by a smaller engine. This in turn reduces the heat loss to the engine and also results in a smaller and lighter car which improves fuel economy.

1.1.3 Effect of Start of Injection (SOI)

Since charge cooling is such an integral aspect of the improved performance of GDI engines, it is important to understand the operation parameters that determine the level of charge cooling. A primary factor in the level of charge cooling is when the fuel is injected into the cylinder, often known as the start of injection (SOI). Injection before IVC improves volumetric efficiency by charge cooling. This allows a larger charge mass at WOT which allows for a small engine. The cooling effect persists with EOI after IVC, and a lower initial charge temperature is produced, which makes knocking less likely. As a result, an increase in the retardation of the spark timing results in a similar increase in the advance of the knock-limited spark timing. If knocking can be avoided then advancing the spark timing results in a larger power output and an increase in engine efficiency.

1.1.4 Vaporization

It is critical that the fuel be entirely vaporized for complete combustion to occur. The results of poor vaporization manifest in multi-phase combustion, lower-exhaust temperatures, higher HC levels, and large levels of soot and particulates. The level of vaporization is primarily a function of the type of fuel, the initial size of the droplets, and the temperature of the air in which the droplets are suspended. The summary of these effects is shown for gasoline in Figure 1-1 [4]. Larger droplet diameters indicate a larger droplet volume which in turn implies a larger mass of fuel to be vaporized. As air temperature increases, the rate of heat transfer from the air to the droplet increases and the rate of droplet vaporization increases which serves to reduce the vaporization time for the droplet. The type of fuel comes into play based upon the latent heat of vaporization which determines how much energy is needed for the fuel to transition from a liquid to a vapor state. A fuel with a larger latent heat of vaporization would have similar relationship between droplet size, air temperature, and droplet life time; however, for the same air temperature and droplet size, the droplet life time would be greater due the higher amount of thermal energy that would have to be transferred.

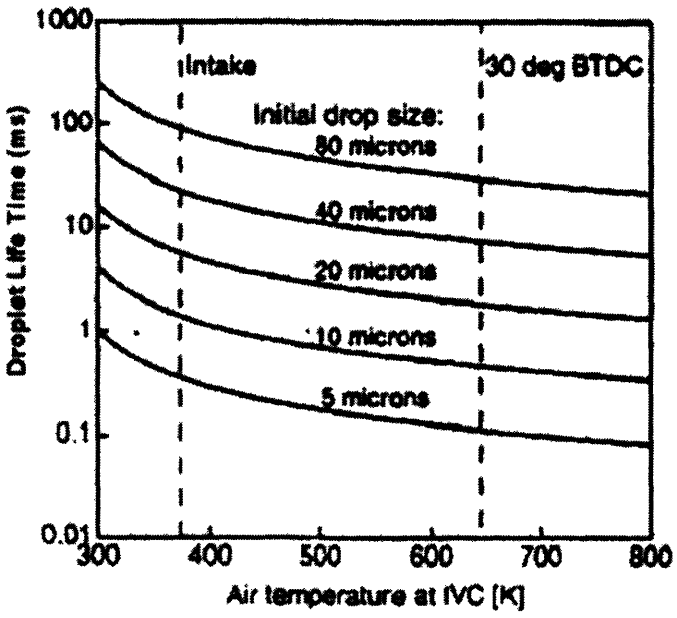

Figure 1-1: Average droplets lifetime vs. air temperature at time of IVC closing. Dashed lines show air temperature at the time of intake valve opening and for 30 CAD bTDC

The type of fuel and the air temperature are mostly indeterminate of engine operation. However, the droplet size if very much a function of the geometry of the injectors and the fuel rail pressure. In general, the droplet size decreased with increasing rail pressure until reaching a steady value. Figure 1-2 [5] shows the Sauter-mean diameter for a Toyota swirl injector. The general trend for almost all types of injectors can be seen in Figure 1-3 [6] in which the dark band is for a large variety of injectors. The chart uses nozzle velocity as the independent parameter, but nozzle velocity can be related to upstream pressure.

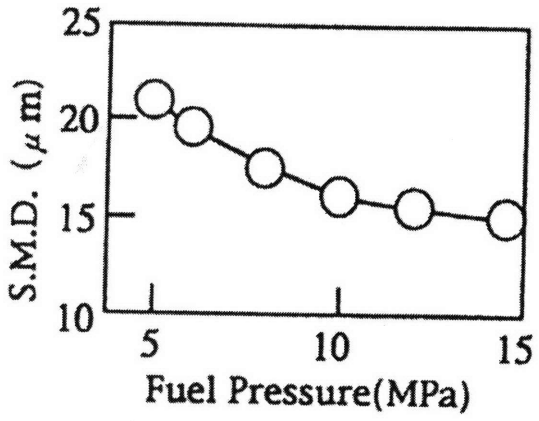

Figure 1-2: Sauter Mean Diameter for gasoline droplets from a Toyota swirl injector as a function of fuel rail pressure

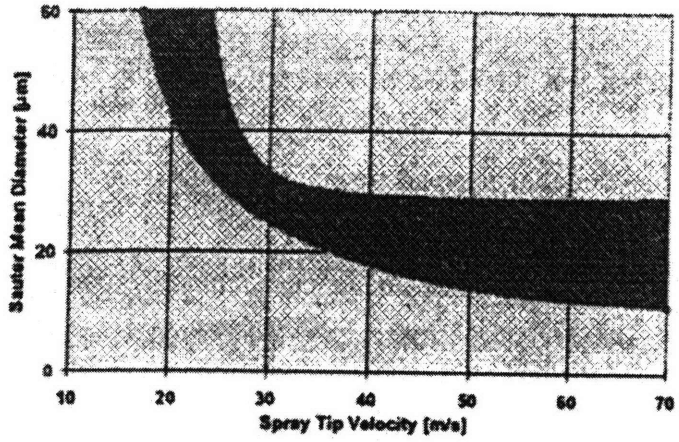

Figure 1-3: Band showing range of Sauter Mean Diameters for gasoline droplets vs. fuel rail pressure

1.1.5 HC Emissions

One of the primary aspects of GDI engines that limit their incorporation into the car fleet is the difference in HC emissions between GDI and PFI engines. The primary reasons for this difference can be summarized in Table 1-2.

Sources of Higher HC Levels	Explanation
Incomplete Vaporization	Fuel that is not vaporized prior to combustion must be vaporized during the combustion event. This alters the combustion event and results in incomplete combustion which produces higher HC levels
Impingement on Cylinder Wall and Piston	The cylinder walls and piston have a large thermal mass and are cooler than the gasses in the cylinder. As such they serve to reduce the rate of vaporization and cool gasses near these surfaces. This results in incomplete combustion and higher HC levels
Entrapment in Lubrication Oil	When the piston moves up and down in the cylinder it leaves a thin film of oil on the cylinder walls. Liquid fuel can become entrapped in this oil film. Once in the oil it is hard for the fuel to evaporate, this is especially true at lower engine temperatures. During combustion, this fuel is ignited, but does not burn cleanly.

Table 1-2: Sources of higher HC levels in GDI engines

1.2 Relevant Formulas

Over the course of the experiments, the operating conditions of the engine would change. As such, the mass of fuel injected and the power output of the engine also varied. In order to normalize the data, the indicated fuel conversion efficiency was used. The simple formula for gross indicated fuel conversion efficiency is shown below [7].

$$\eta_{i,g} = \frac{\dot{W}_{i,g,engine}}{\dot{W}_{chemical,fuel}}$$

The efficiency represents the percentage of the chemical energy of the fuel which is converted to mechanical energy. A common way to measure the mechanical energy of an engine is the mean effective pressure. A common definition of work is:

$$W = \int_{V_1}^{V_2} PdV$$

As such, the average pressure that occurs over a change in volume can be found by dividing the energy produced by the change in volume that resulted in that work output. In a four-

stoke engine, an engine cycle requires two rotations of the engine. This results in the following formula for mean effective pressure.

$$MEP = \frac{\dot{W} \bullet 2}{N \bullet V_{disp}}$$

Different forms of MEP exist. One definition takes power output to be the power output indicated by the pressure in the cylinder vs. time. This is known as the indicated mean effective pressure (IMEP).

$$IMEP = \frac{\int_{V_1}^{V_2} PdV}{V_{disp}}$$

Two forms of IMEP exist. For net indicated values, V_1 and V_2 are both defined to be the minimum volume of the cylinder so that the integration is from BDC of the compression stroke through two engine revolutions and back to BDC of the compression stroke. For gross indicated values the integration is only done from BDC of the compression stroke to BDC of the expansion stroke. As such, the gross indicated value does not account for work losses to the difference in pressure between the exhaust and intake stroke. In order to remove the effect of changes in exhaust pressure due to the trench fans, the gross indicated pressure was used rather than the net indicated pressure. The above formulas were thus re-arranges to yield the following formula:

$$\dot{W}_{i.g.\ engine} = \frac{GIMEP \bullet N \bullet V_{disp}}{2}$$

The theoretical maximum work based upon the mass of fuel injected was found using the formula below in which LHV is the lower heating value of the fuel.

$$\dot{W}_{chemical,\ fuel} = \dot{m}_{fuel} \bullet LHV_{fuel}$$

2 Experimental Setup

In order to examine the effects of different parameters on emissions in a DISI engine, a production 2005 GM Ecotec engine was used. The engine originates from GM's European Opal division [8]. The engine has a four-cylinder inline layout and has a maximum power-output of 155 hp at 5600 RPM. The relevant geometric and timing values are listed below.

Displacement, V_d	**2198 cm^3**
Bore, B	**86.0 mm**
Stroke, L	**94.6 mm**
Compression Ratio, r_c	**12.0**
IVO / IVC	**0° aTDC / 60° aBDC**
EVO / EVC	**44.5° bBDC / 10.5° aTDC**

Table 2-1: Engine Geometry and Valve Timing

The valve timing in this engine can be compared to those in a similar Ecotec PFI engine which has an IVO / IVO timing of 7° bTDC / 56° aBDC and an EVO / EVC timing of 68° bBDC / 16° aTDC [8]. It is clear that the two engines have different valve timings. However, the DISI engine was originally designed for a European market in which less stringent emissions standards exist and it is not uncommon for lean combustion in direct injection engines. As such, when the engine was modified for homogenous stoichiometric combustion it seems likely that the result was a significantly different valve timing than would be found in a PFI injection engine which had always been designed for homogenous stoichiometric combustion [8].

As previously stated, the engine is intended for spark induced combustion of a homogenous stoichiometric mixture of gasoline and air. As such, the piston, as shown in the

image below, is of a standard flat geometry with little to no surface features. If the engine was to be made able to run in lean mode, the piston would have be replaced with a piston whose topography would allow the injected fuel charge to be guided to create stratification.

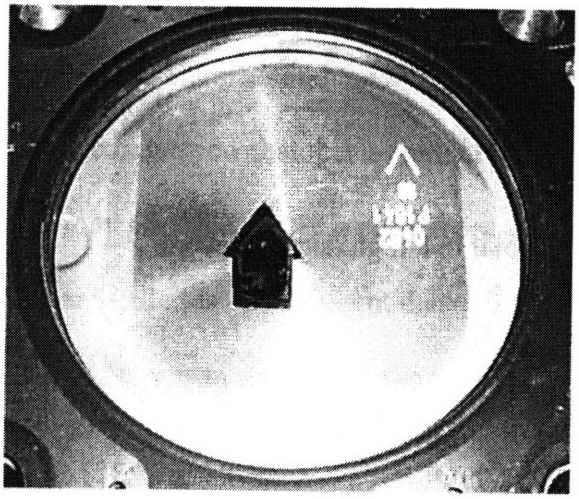

Figure 2-1: Image of top surface of piston

An image of the engine head can be seen below [8]. The engine has two intake valves located on the left hand side of the image and two exhaust valves located to the right hand side of the image. All valves are operated under the fixed cam timing mentioned above. Located in the center of the header, between all four valves, is the spark plug. To the far left is the opening for the nozzle of the injector. The engine uses a single-hole Siemens DAKU injector which can be operated with an upstream fuel pressure of 40 – 120 bar. The injector makes an angle of 47° with respect to horizontal and has a nominal cone angle of 52°. A schematic of the nominal set-up of the injector is shown in Figure 2-3 [9]; the actual cone will not conform to such a simple shape.

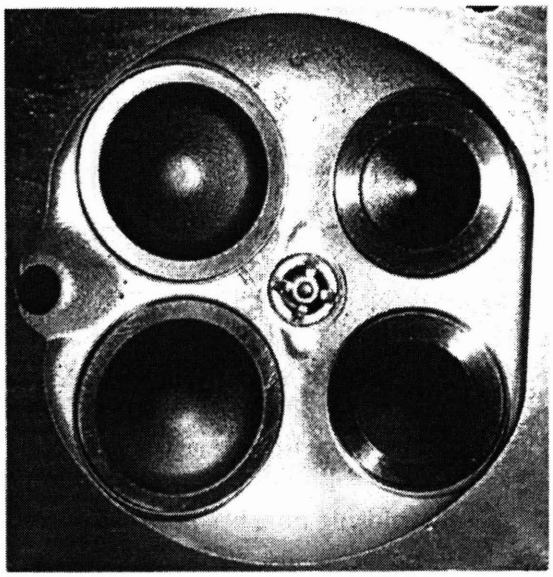

Figure 2-2: Image of the engine head showing the intake and exhaust valves as well as the spark plug and injector locations

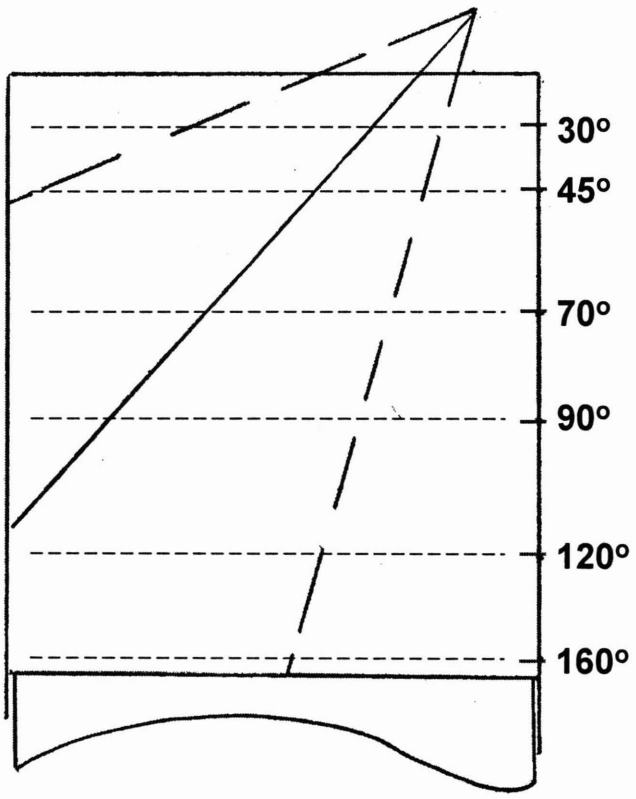

Figure 2-3: Piston position and spray pattern for engine

The combustion in any given cylinder does not depend on the combustion in other cylinders. As a result, the engine was run with only one cylinder in order to reduce the complexities of interpreting the data. This required a modification of the intake and exhaust systems as well as the injection and firing systems. The intake and exhaust runners for one cylinder was isolated from the intake and exhaust manifolds and connected to independent systems. A schematic of the modified system can be shown below. It should be noted that this system allowed the air entering one cylinder to be measured and also to ensure that all emissions in the exhaust mixing tank came from that cylinder.

2.1 Instrumentation

Several high precision instruments were used to control the engine and measure operating parameters.

2.1.1 In Cylinder Pressure Transducer

A Kistler 6125A pressure transducer was used to measure the cylinder pressure. This particular sensor was chosen because of its fast response and because it is the sensor recommend by industry and academics for this type of application. In order to measure cylinder pressure, the sensor had to be mounted inside the engine head. It was very important that this complex machining be done precisely. The machined section had to reach a precise depth in order to minimize the separation between the tip of the sensor and the combustion chamber to ensure a fast and accurate response. At the same time it was critical that the contour of the combustion chamber and its structural integrity not be compromised or else the potential existed for a catastrophic mechanical failure which would not only damage the engine but also pose a risk to anyone near the engine. It was also important to properly isolate

the pressure transducer from coolant and oil galleries. Due to the complexity and tight tolerances of this machining, it was performed by GM at their facilities. In addition, to allow for the possibility of at a later time running on all four cylinders or testing on a different cylinder, the header above all four cylinders was machined to accept a pressure transducer probe.

After several early experiments it was found that the pressure trace demonstrated erratic behavior that could not be explained. It was determined that the probe had suffered some thermal damage and needed to be replaced. The possibility of a thermal screen being used was also discussed; however the small porosity of the screen would prevent a fast and accurate measurement of the cylinder pressure [8]. As such, no thermal screen was implemented, but the pressure data from each round of testing is checked to insure that the sensor has not suffered any thermal damage or is showing any erratic thermal drift.

The pressure transducer has a sensitivity of 13.7 pC/bar with a linearity of +/- 0.5% of the full scale [8]. The pressure sensor is a relative measurement device, as such to determine the pressure in the cylinder, the output of the sensor at a given time must be pegged to a known value. This is done through the use of a secondary pressure sensor located in the intake manifold which records the MAP. The output of the pressure transducer at BDC of the intake stroke is "pegged" at the pressure determined by the pressure sensor in the manifold. The linear relationship between pressure and the output of the pressure transducer then allows the change in pressure to be found which is then added to the MAP to determine the cylinder pressure.

2.1.2 Lambda Meter

To acquire air/fuel ratio information, an Etas LA4 Lambda meter was located 17 cm from the exhaust port. The meter utilizes a Nernst concentration cell and an oxygen ion pump cell. The meter is has a planar two cell design with one layer composed of a solid body multilayered ceramic electrolyte which separates a reference gas and the exhaust. The difference in oxygen concentration between the reference gas and the exhaust is a function of the air/fuel ratio of the combustive mixture in the cylinder. A voltage is induced across the electrolyte which is very sensitive to the difference in oxygen concentration. The precise measuring of this voltage allows the lambda sensor to determine the lambda value in the cylinder.

2.1.3 Fast Flame Ionization Detector (FFID)

To acquire data on the levels of HC emissions a Cambustion HFR-400 Fast Flame Ionization Detector was used. The FFID has a time response (10 – 90%) of approximately 1 millisecond [8]. The FFID works by sampling the exhaust stream and passing it through a hydrogen flame. The resulting flame consumes all unburned hydrocarbons resulting in the emissions of particular hydrocarbon ion. A fast response ion detector produces a voltage signal proportional to the ion current. The instrument is calibrated by using ambient air to zero the readings. A calibration gas composed of 1520 ppm propane (C_3H_8) and inert nitrogen gas was used. The 1520 ppm concentration of propane corresponds to a 4560 ppm concentration of C_1 which was used to find the scaling factor which was then inputted in the data logging software. Emissions from a well mixed, large volume dampening tank located 180 cm from the exhaust port were sampled to find the average level of HC emissions

corresponding to the running conditions. In addition another sampling probe was placed 15 cm from the exhaust port to record the instantaneous HC emissions.

2.2 System

The system has been divided into its different functional subsystems in order to better explain the overall system. A picture of the actual test set-up is shown below.

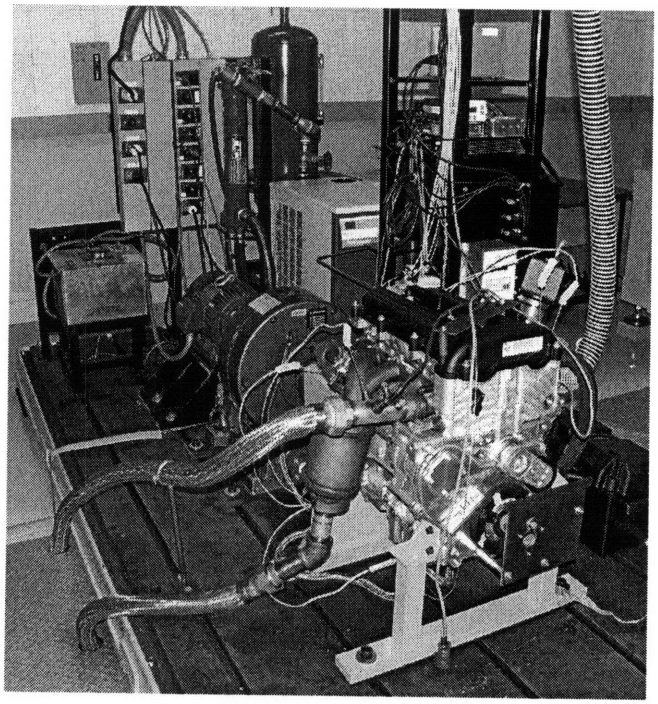

Figure 2-4: Image of engine set-up

2.2.1 Intake System

A schematic of the intake system is shown below. Air from the room passes through a filter and then through the air flow meter which measures the mass of the entering air. Since all experiments are steady state, it was assumed that the mass of air entering the intake system would correspond to the mass of air entering the cylinder. In addition, the experiments being steady state made a throttle unnecessary and too prone to variation. In place of the throttle the flow went through two parallel gate valves, one for fine control and one for broad control. In

theory any MAP can be achieved with this system. However, the experiments focused on the fast idle condition and so the MAP was never set above 0.5 bar and most often at around 0.29 bar.

Downstream of the parallel valves was a large mixing tank which served to smooth out the pressure oscillates due to the periodic nature of the flow of air into the cylinders. The tank has a volume of 10 liters which is a factor of 20 larger than the maximum displaced volume of the active cylinder. The hose connecting the tank to the intake for the active cylinder is rated to a full vacuum (22.9 mm Hg) and has a smooth inner contour. At the connection between the hose and intake runner, the hose is held in place with a wire clamp and sealed with silicone tape. A thermocouple was used to measure the temperature of the air entering the intake. A schematic of the system can be seen below.

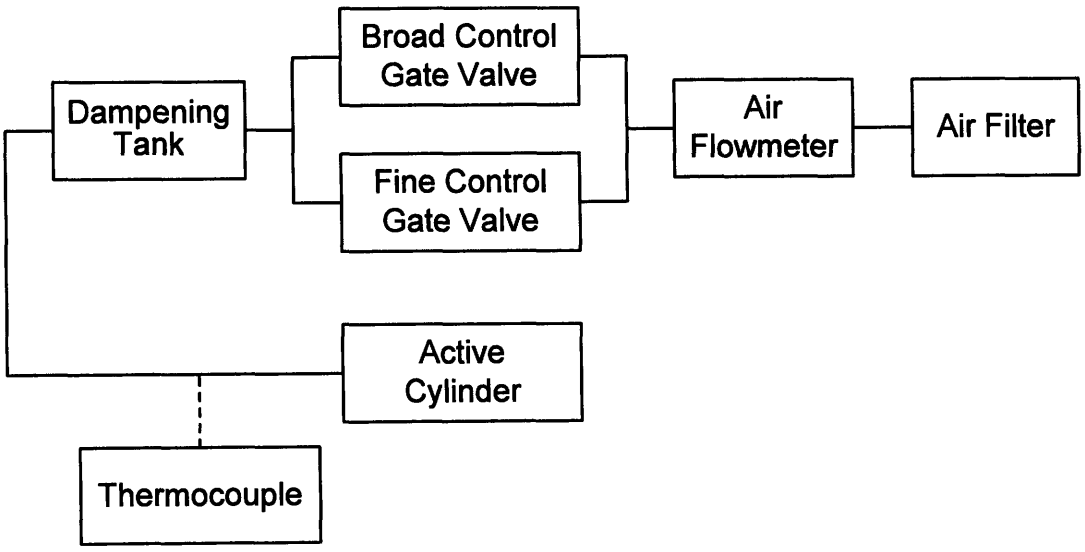

Figure 2-5: Schematic of Intake System

2.2.2 Fuel System

The fuel system has undergone a series of modifications from the original system. The stock engine uses a mechanical fuel pump driven by the camshaft to pressurize the fuel prior to injection. However, in order to maintain a constant injection pressure that was independent of engine speed or other parameters, a new set-up was created. A simple schematic of the most basic system is shown below. A small electric pump is used to draw fuel from the fuel tank and pump the fuel through a fuel filter and past a three-way valve and into a hydraulic accumulator.

The hydraulic accumulator is a high pressure cylinder with an internal piston. As the fuel is pumped into the cylinder, the piston rises with the level of fuel until the piston reaches its upper stops. A high pressure nitrogen bottle with a maximum pressure of 160 bar is connected through a manual pressure regulator to the top of the accumulator. The pressure regulator allows nitrogen gas to enter the accumulator until the desired pressure is reached at which point flow stops. The nitrogen gas applies pressure to the top of the piston which in turn pressurizes the fuel. As fuel is injected into the cylinder the fuel level falls and additional nitrogen gas enters the top of the accumulator to maintain the pressure.

The two way valve is closed before the system is pressurized and prevents the fuel from being forced backwards through the fuel pump and into the fuel tank. The bottom of the fuel accumulator is also attached to the fuel rail. With the fuel unable to travel back into the fuel tank, the pressurized fuel from the accumulator enters the fuel rail where it is injected into the active cylinder through the high pressure injectors. The system is limited to an operating pressure of 135 bar (2000 psi) by the strength of the stainless steal tubing which

were used for the high pressure lines. Since the lines are stainless steal there is little potential for corrosion by the ethanol fuels.

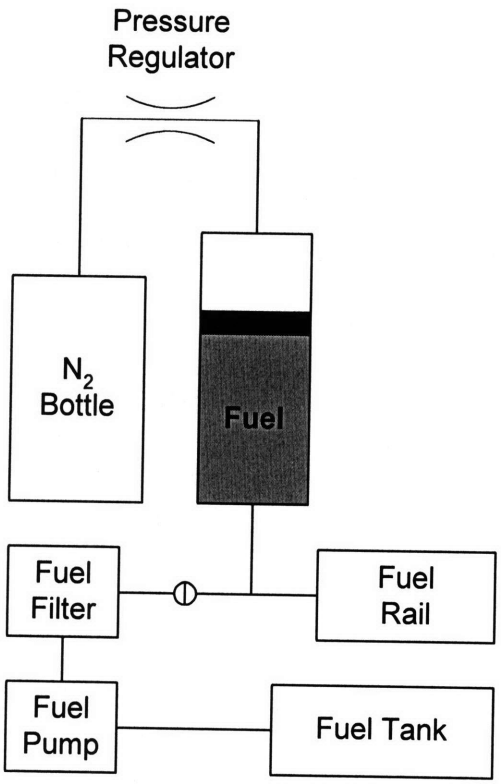

Figure 2-6: Schematic of fuel system concept

The system described above works well when only one fuel is to be tested. However, it was determined that in order to minimize contamination and isolate the ethanol blends from the gasoline, it was important to have different accumulators for each type of fuel and also to have the gasoline system be isolated as much as possible from the ethanol blends. The resulting system schematic is shown below. Several key features should be noted. A KNF model N726FTP diaphragm vacuum pump is used to remove air and/or residual fuel from the fuel system during the filling of accumulators and during fuel changeovers. The pump is able to produce a vacuum up to 28 in. Hg and uses a Teflon diaphragm rather than pumping oil to

produce a vacuum, as such there is no potential for fuel vapors damaging the pump. A 4-liter Erlenmeyer flask is used as a liquid trap to prevent liquid fuel from entering the vacuum pump where it would inhibit the proper functioning of the pump.

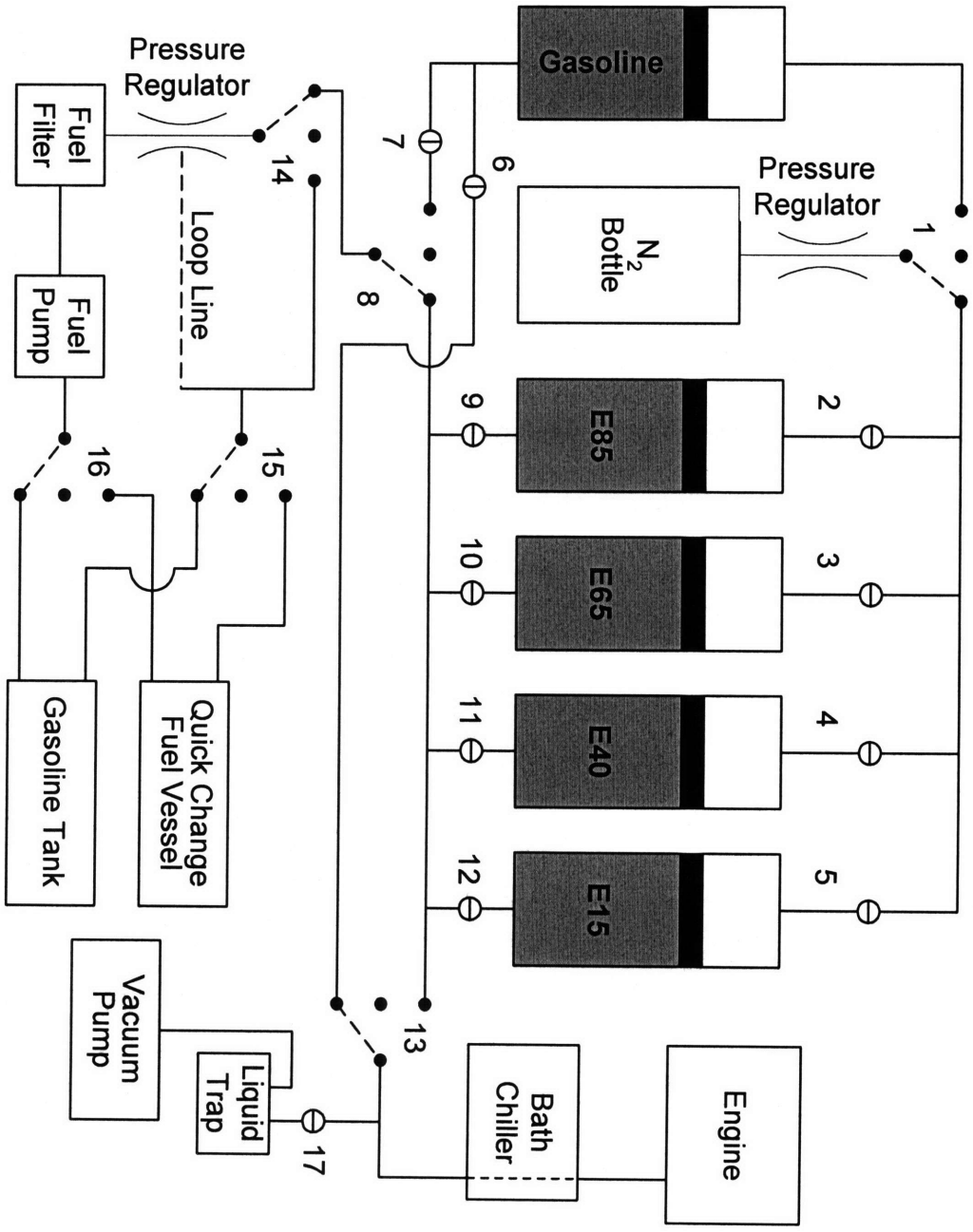

Figure 2-7: Schematic of entire fuel system. Valves are numbered solely for reference

The injectors were calibrated as a function of fuel type and difference in pressure across the injectors through the use of a custom rig. The rig allowed the fuel rail and injectors to be mounted outside the engine. A custom program was used to fire the injectors for several hundred cycles of fixed duration. The injected fuel was captured in a sealed glass jar which was cooled in an ice bath to minimize vaporization. The jar was weighed before and after each round of injections to determine the mass of fuel corresponding to the number and duration of the injections. The calibration curves can be seen in Appendices 1, 2, 3, and 4.

2.2.3 Coolant System

A special system was designed to control the temperature of the engine coolant over a broad range of temperatures. The coolant system was divided into two loops, one for low temperature tests and one high temperature test. A schematic of the system is shown below [8].

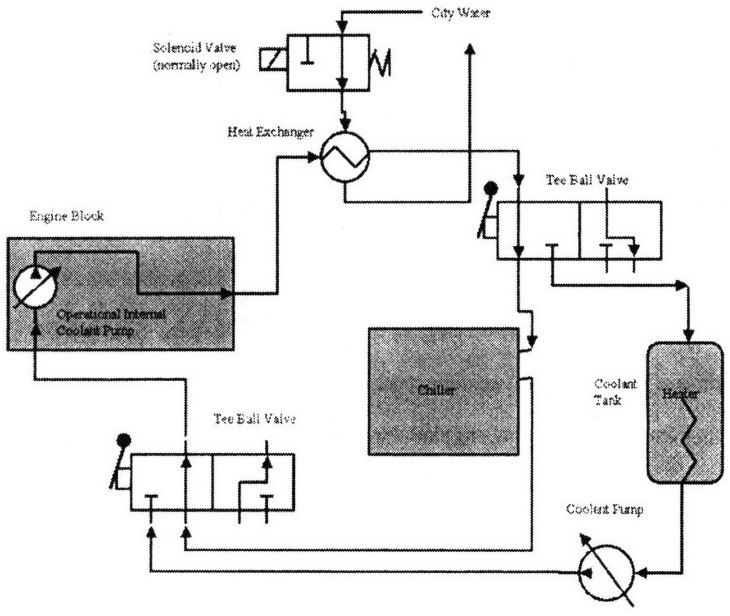

Figure 2-8: Schematic of system for controlling the coolant temperature

The heating system utilizes a large coolant tank containing a 10 kW electric heater. The low temperature system employed a small chiller. When the heating loop was used, the coolant returning from the engine would enter the large coolant tank where it would be heated by the electric heater; 80° C was set as the maximum coolant temperature to prevent damage to the engine or over pressurizing of the coolant tank or lines. The low temperature system was to have coolant temperature reduced by the chiller. However, the chiller did not have a high enough capacity to compensate for the thermal energy gained from the engine and the environment as the coolant flowed through the coolant lines. An additional problem is that the internal coolant pump of the engine could not be disengaged because it was driven by a chain drive within the engine and the chiller only had a small reservoir intended for low flow rates. As such, the pump within the chiller was overwhelmed by the engine pump and the coolant was not properly cooled. The lowest temperature that could be reliable tested was 20° C during the fall and winter seasons and 33° during the spring and summer.

Regardless of which system was being used, the temperature of the coolant was maintained through the use of a simple control system connected to a solenoid valve which controlled the flow of city water through the heat exchanger. When the heating system was operating, two set-points were used to bracket the desired temperature. If the coolant temperature was less than the first set-point then the electric heater would be activated to increase the coolant temperature. If the coolant temperature exceeded the second set-point then the solenoid would close and allow city water to flow into the heat exchanger where it would serve to reduce the temperature of the coolant. During low temperature tests only the second set-point was used and the electric heater was disconnected. The chiller was set to the lower limit on the temperature and attempted to chill the coolant to that temperature. If the

temperature became to low then the solenoid valve would close and city water would enter the heat exchanger where it would serve to increase the temperature of the coolant. The system was able to maintain the temperature within +/- 5° C of the desired temperature as long as the operating temperature was between 20° and 80° C.

2.2.4 Exhaust System

The exhaust system was also modified so as to isolate the exhaust from the active cylinder from the remaining three cylinders. The lambda sensor, FFID probe, and a thermocouple are all approximately 15 cm from the exhaust port. A mixing tank is located 180 cm from the exhaust port and allows for the average concentration of carbon monoxide and hydrocarbons to be measured. A rubber burst disc on the mixing tank prevents the mixing tank from bursting if a misfire occurs. Exhaust is allowed to flow from the mixing tank into the trench beneath the test cell where blowers remove the exhaust. Although the blowers assist in the blowdown process, the large volume of the mixing tank minimizes the effect on exhaust pressure.

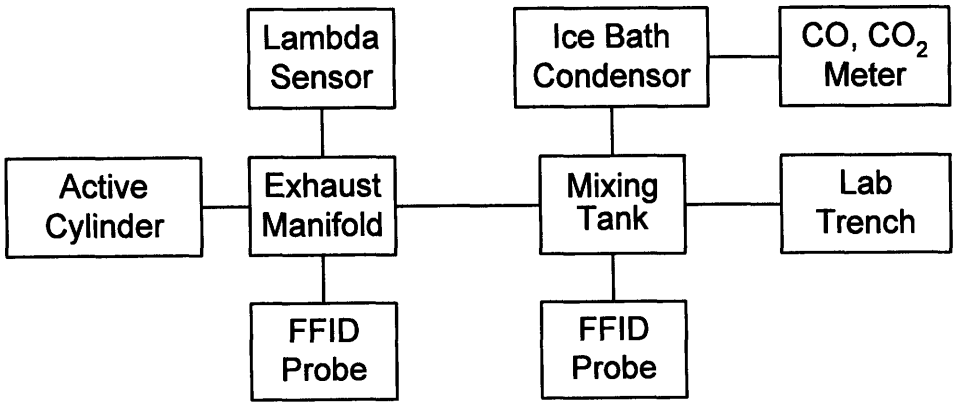

Figure 2-9: Schematic of Exhaust System

2.2.5 Charge Motion Control Valve (CMCV)

As previously stated, the engine has two intake ports. However, in order to maximize mixing while allowing for the engine to effectively operate at wide open throttle, the engine employs a charge motion control valve (CMCV). A depiction of the CMCV and the resulting air flow patterns as well as a picture of the CMCV are shown below in Figure 2-10 and Figure 2-11 [9]. The engine is designed with one intake port coming in perpendicular to the motion of the piston. The other intake port is oriented to closer to parallel to the motion of the piston. As low speeds, the CMCV is closed which blocks the intake port parallel to the piston motion. The entire charge is forced to flow through the perpendicular intake port which results in the charge having a swirling motion which is better for mixing at low speeds. At higher loads and consequential higher engine speeds, the CMCV is opened and the air charge can flow through both intake ports resulting in a tumbling charge motion which results in a smaller head loss. It is important to note that the actual charge motion is not as simplistic and regimented as shown in the figure.

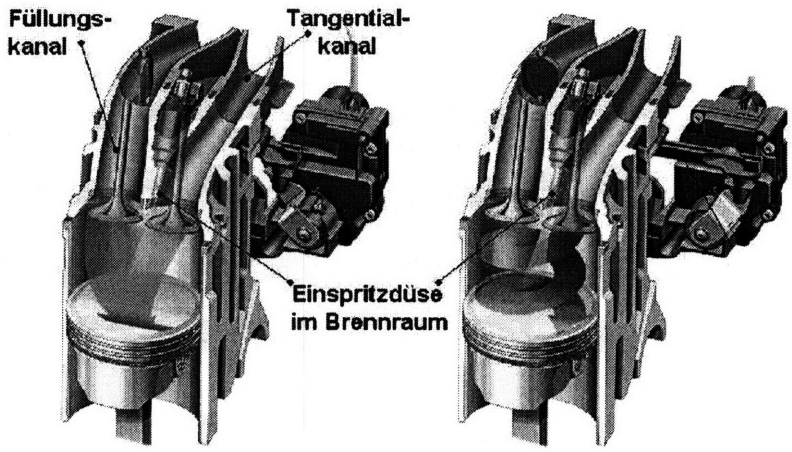

Figure 2-10: Depiction of Charge Motion Control Valve and resulting flow patters

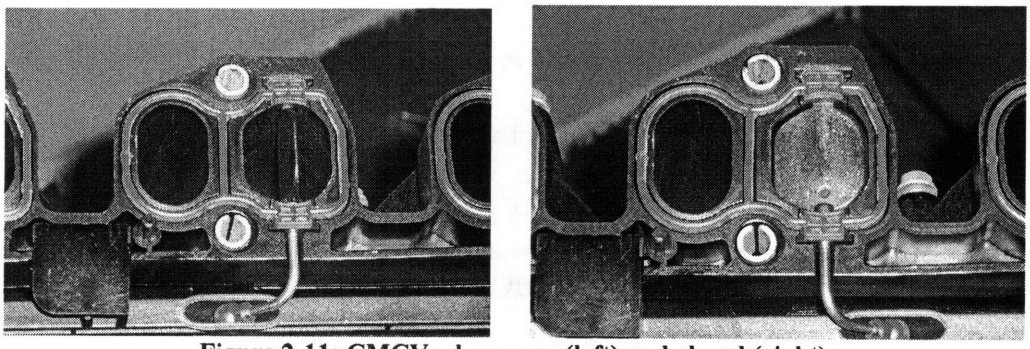

Figure 2-11: CMCV when open (left) and closed (right)

2.2.6 Engine Control System

The injection and firing of the spark plug is controlled through a master and a slave computer. The master computer program can be run out of a DOS command prompt in Windows. The master computer takes the users input on engine speed (RPM), the target lambda value, spark timing (CAD aBDC compression), and end of injection (CAD aBDC compression). Using the engine speed it calculates the amount of time that the spark plug needs to be charged before it can fire which is referred to as the dwell time. This information and the other variables are placed in an array and passed to the slave computer. While the master program is running it will accept new values for the target lambda, spark timing, and end of injection from the user and pass these new values to the slave computer.

The slave computer is the computer that actually runs the engine. Before the program runs it takes three inputs. The first two inputs are the proportional and integral feedback coefficients. In order to achieve and maintain the desired lambda value, the program must constantly adjust the duration of the fuel pulse. This is done through the use of a feedback control loop which uses the output of the exhaust lambda sensor. Originally only proportional feedback was used. However, this resulted in a harmonic lambda response in which the

lambda value oscillated around the desired value. Since emissions can vary significantly with lambda, it was important to reduce this error. As such, integral feedback was incorporated into the feedback system to damped the response and reduce the error in lambda. The coefficients simply serve to set the level of proportional and integral feedback. The last input is injection duration for the first engine cycle. In all subsequent cycles the lambda feedback system will adjust the fuel pulse duration to the desired value. A plot showing the lambda value for each cycle with and without the integral feedback is shown below.

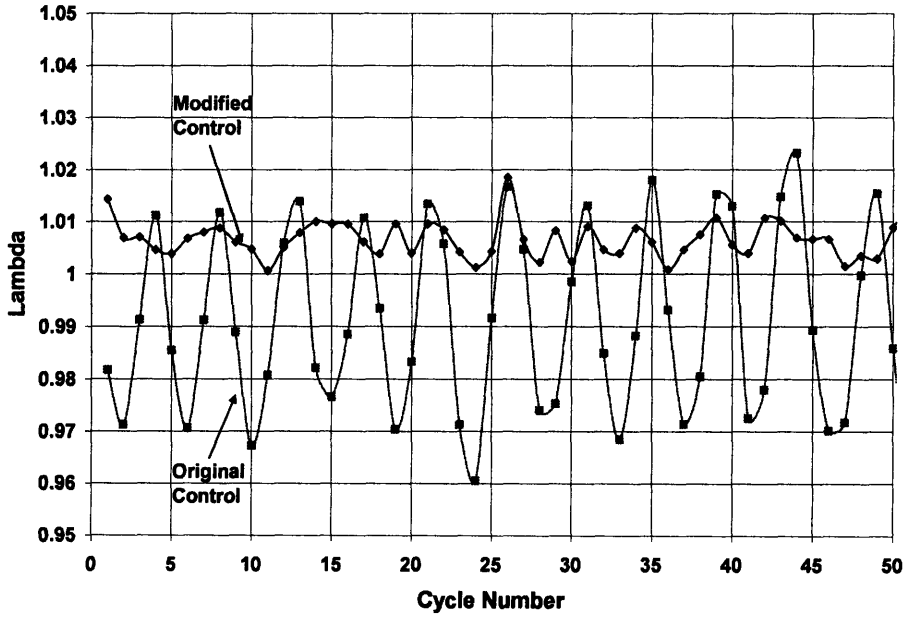

Figure 2-12: Measured lambda for 50 consecutive cycles with and without the integral feedback

While the slave computer is running it has to do many things very quickly. The slave computer has to charge and fire the spark plug, calculate the fuel pulse duration, activate the injectors at the right time and for the correct duration, and output a voltage proportional to the fuel pulse duration which is used by the data acquisition system. Every cycle the slave computer also checks for an updated array for variables from the master computer and adjusts

its operation accordingly. Since all these tasks must be performed quickly and reliably, it is not possible to run the computer in Windows which uses the processor and memory to track mouse movement and run other programs. The delay caused by these actions would result in unpredictable engine operation and dangerous misfires. The slave computer program can be ended with a hardware switch which interrupts the program and ensures that the sequence of firing and injecting is stopped with the injectors closed and the spark coil discharged to prevent fuel from entering the cylinder or a misfire.

2.2.7 Data Acquisition System

The Data acquisition system is modeled on a National Instruments platform. The schematic is shown below in Figure 2-13 and a list of the components and their function is provided in Table 2-2 [8]. Several thermocouples have been integrated into the engine to measure properties such as intake and exhaust temperature, coolant temperature and fuel temperature. However, the time response of the thermocouple hardware is not sufficient to allow the data to be logged at the speed at which the engine is running. Since only the steady state value of these properties was relevant, the thermocouples were simply connected to an Omega thermocouple reader which allowed the steady state temperature to be determined.

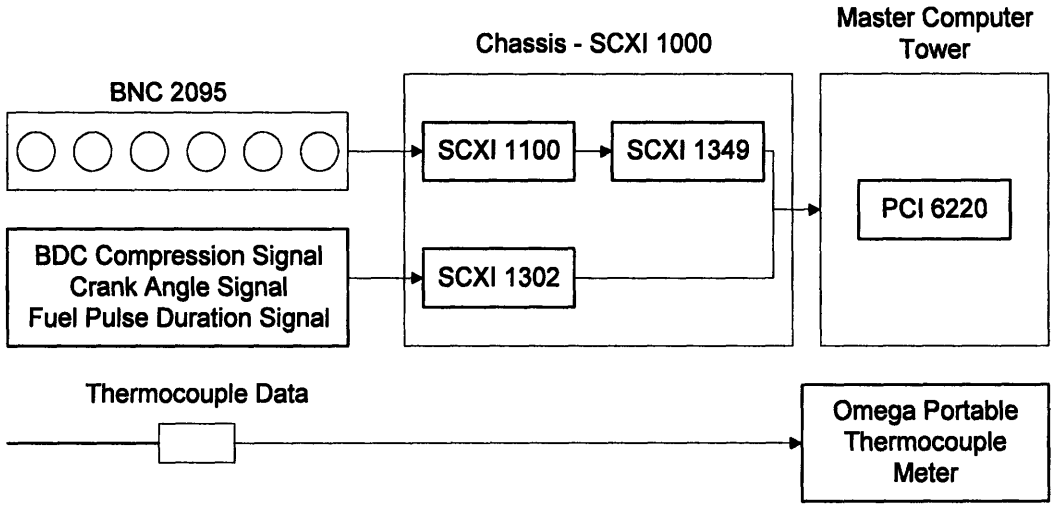

Figure 2-13: Data acquisition system

Item	Function
BNC 2095	Records up to 16 different analog BNC signals
SCXI 1100	Multiplexes the signal into a single programmable gain instrumentation amplifier (PGIA)
SCXI 1302	Allows digital signals to feed through to the master computer
SCXI 1349	Necessary adaptor to include feed through signals
PCI 6220	Data acquisition card

Table 2-2: Components and functions for data acquisition system

2.3 Operating Procedures

In order to ensure repeatability between experiments and to properly operate the system, operation procedures were developed and are described in the tables below.

Filling accumaltor when same fuel is to be used	
1	Depressurize the nitrogen lines by turning the pressure regulator knob counterclockise several times until it feels loose. Regulator pressure will rapidly fall and be accompanies by a hissing sound as the gas in the system is pushed passes the relief valve in the regulator.
2	When regulator pressure registers as 0 and hissing has subsided, turn 3-way valve (1) near regulator to set system pressure to ambient.
3	Ensure that enough fuel remain in the fuel container. Failure to do will result in air in lines which will have to be purged.
4	Either remove blue cap from top of gasoline tank or remove weight from top of quick change over container to allow air to enter as fuel is pumped out of fuel container.
5	Set 3-way valve (13) to "fill" and make sure that the second 3-way valve (8) is open and selecting the correct tower.
6	Flip the fuel pump switch at the front control panel. Pressure will be approximately 25 psi while filling. Eventually pressure will rapidly rise to 80 psi and open the relief valve on the pressure regulator and send all subsequent fuel back the fuel container through the loop line.
7	Turn off fuel pump at front control panel.
8	Set first 3-way valve (14) to closed and turn second 3-way valve (8) so that neither tower is selected
9	Return blue cap or weight to the fuel container. This will prevent vapors from being vented from container.
10	Turn 3-way valve (1) near gas pressure regulator back to the original position to allow nitrogen gas to flow from the regulator to the top of the accumulators.
11	Turn the regulator knob clockwise slowly until the desire pressure is reached. There will be pressure losses in the system due to head losses and piston friction. As such the regulator presure will have be set above the desired fuel rail pressure.

Table 2-3: Filling accumulator with same fuel

Fuel changeover from one ethanol blend to a different ethanol blend	
1	Depressurize the nitrogen gas lines using the pressure regulator knob and the 3-way valve (1).
2	Close the valve beneath the accumaltor containing the fuel that was being used (9, 10, 11 or 12).
3	Open the valve (17) connecting the fuel system to the vacuum pump.
4	Turn on the vacuum pump and allow fuel to flow into the fuel trap.
5	When fuel flow stops, lift rubber stopper on fuel trap to return fuel system to ambient pressure.
6	Reseat the rubber stopped and once again run vacuum pump for 10 - 15 seconds or until desired level of vacuum is reached.
7	Close valve above accumalor containing fuel that was being used (2, 3, 4, or 5). Open valve above accumulator containing new fuel (2, 3, 4, or 5). This will allow the accumulator piston to move freely.
8	Open valve to accumulator containting new fuel to be tested (9, 10, 11 or 12). There will be a rapid flow of fuel into the liquid trap. When no air appears in fuel entering liquid trap, close valve (17) connecting fuel system to vacuum pump.
9	Fuel system will now contain new fuel.
10	Set the 3-way valve (1) into the correct position and repressurize system to desire pressure using the gas presure regulator

Table 2-4: Procedure for changeover to ethanol blend from a different ethanol blend

Fuel changeover from gasoline to an ethanol blend	
1	Depressurize the nitrogen gas lines using the pressure regulator knob and the 3-way valve (1).
2	Close valves (6 and 7) below accumalor containing gasoline.
3	Make sure that all valves (9, 10, 11 and 12) below the ethanol blend accumalators are closed.
4	Turn 3-way valve (13) such that now selects the ethanol blend tower rather than the gasoline tower.
5	Set 3-way valve (1) so that nitrogen gas can flow to the ethanol accumulators
6	Open the valve (17) connecting the fuel system to the vacuum pump.
7	Turn on the vacuum pump and allow fuel to flow into the fuel trap.
8	When fuel flow stops, lift rubber stopper on fuel trap to repressurize system to ambient pressure.
9	Reseat the rubber stopped and once again run vacuum pump for 10 - 15 seconds or until desired level of vacuum is reached.
10	Open valve (2,3,4 or 5) above accumulator containing new fuel to be used
11	Open bottom valve (9, 10, 11 or 12) to accumulator containting new fuel to be tested. There will be a rapid flow of fuel into the liquid trap. When no air appears in fuel entering liquid trap, close valve (17) connecting fuel system to vacuum pump.
12	Repressurize system to desire pressure using the gas presure regulator

Table 2-5: Procedure for changeover to ethanol blend from gasoline

Filling an ethanol blend accumaltor when previosuly filled system with a diffent fuel	
1	Depressurize the nitrogen gas lines using the pressure regulator knob and the 3-way valve (1).
2	Close all bottom valves (6, 7, 9, 10, 11 and 12) for accumaltors.
3	Place a small amount of the new fuel in the quick change fuel container (~1.5 liters)
4	Ensure that both 3-way valves (8 and 14) are closed.
5	Turn on fuel pump, with both 3-way valves (8 and 14) closed this will immediately cause the pressure relief valve to open. This will cause all of the fuel that was in the system up to valve (14) to be slowly purged from the system through the "loop line". Depending on acceptable level of cross-contamination, multipe flushes can be done.
6	Dump fuel in the quick change fuel vessel into an acceptable waste fuel container.
7	Fill quick change fuel vessel with at least 4 liters of new fuel.
8	Make sure that 3-way valve (13) is seleting the ethanol blend tower.
9	Open the valve (17) connecting the fuel system to the vacuum pump.
10	Turn on the vacuum pump and allow fuel to be sucked in the fuel trap.
11	When fuel flow stops, lift rubber stopper on fuel trap to repressurize system.
12	Reseat the rubber stopped and once again run vacuum pump for 10 - 15 seconds or until desired level of vacuum is reached.
13	Set 3-way valve (1) so that it selects the ethanol tower.
14	Open both 3-way valves (8 and 14), making sure the second 3-way (8) is selecting the ethanol tower. Vacuum will cause new fuel to be sucked into the fuel lines and fuel will enter the liquid trap and in the process purge the remaining old fuel.
15	Close valve (17) connecting vacuum pump to the fuel system once old fuel and any air have been flushed.
16	Open bottom (9, 10, 11 or 12) and top valve (2, 3, 4 or 5) on accumaltor to be filled and close top valve (2, 3, 4 or 5) on accumulator that was used before.
17	Turn on fuel pump at front panel and when accumlator is full turn off fuel pump
18	Close both 3-way valves (8 and 14) and repressurize the system

Table 2-6: Procedure for filling an ethanol blend accumulator when previously filled a different accumulator

Filling the gasoline accumulator when previously filled an ethanol blend accumulator	
1	Depressurize the nitrogen gas lines using the pressure regulator knob and the 3-way valve (1).
2	Close all bottom valves (6, 7, 9, 10, 11 and 12) for all accumaltors.
3	Place a small amount of gasoline in the quick change fuel container (~1.5 liters)
4	Ensure that both 3-way valves (8 and 14) are closed.
5	Turn on fuel pump, with both 3-way valves (8 and 14) closed this will immediately cause the relief valve to open. This will cause all of the fuel that was in the system up to those valves to be slowly purged from the system through the "loop line". Depending on acceptable level of cross-contamination, multipe flushes can be done.
6	Dump fuel in the temporary storage device into an acceptable waste fuel container.
7	Have 3-way valve (8) selecting the ethanol tower.
8	Open the valve (17) connecting the fuel system to the vacuum pump.
9	Turn on the vacuum pump and allow fuel to be sucked in the fuel trap.
10	When fuel flow stops, lift rubber stopper on fuel trap to repressurize system.
11	Reseat the rubber stopped and once again run vacuum pump for 10 - 15 seconds or until desired level of vacuum is reached.
12	Turn the two ball valves (15 and 16) on the blue hoses to select the gasoline tank. (Note: It is done this way because if you used the gasoline tank to purge the pumping system then ethanol would end up in the gasoline tank and the entire tanke would have to be purged and flushed with gasoline.)
13	Turn the tower selector valve (8) so that in now selects the gasoline tower and open the bottom valves (6 and 7) for the gasoline accumulator.
14	Set the first 3 way valve (14) to "fill". Vacuum will cause gasoline to be sucked into the fuel lines and gasoline will enter the liquid trap and will remove any remaining old fuel.
15	After system is properly flushed of olf fuel and air, close valve (17) connecting vacuum pump to the fuel system.
16	Set valve (1) to select the gasoline accumulator and close top valve (2, 3, 4, or 5) on accumulator that was used before.
17	Turn on fuel pump at front panel and when accumlator is full turn off fuel pump.
18	Close both 3-way valves (8 and 4) and valve (7) below accumulator and repressurize the system
19	Repressurize the system using the pressure regulator for the high pressure nitrogen bottle

Table 2-7: Procedure for filling the gasoline accumulator when previously filled an ethanol blend accumulator

Engine Motoring	
1	Turn on lab fan and water pump using the two button switches
2	Make sure all valves are in correct position, especially that valves ( ) are closed to prevent a pressurized backflow of fuel
3	Allow flow from the nitrogen bottle by turning the top knob clockwise. Make sure you open the valve completely to maximize the rate of nitrogen gas flow.
4	Pressurize the nitrogen line by turning the pressure regulator kbob clockwise
5	Ensure the National Instrumens chassis is powered
6	Flip the motor breaker to the "on" position and allow 5 minutes for warm up
7	Check around the motor, dyno, and other rotating parts for wires and other obstructions
8	Check the oil level with the dipstick and check the coolant levels in the reservoir tank
9	Ensure the coolant flow valves are in the proper position
10	On the wall adjust the ball valves directing the flow of water to the dynamometer, coolant heat exchanger, and oil heat exchanger. The dynamometer valve should be completely open. The coolant valve position depend on the temperature at which the engine is to be run, with the valve only cracked at high temperatures and slighly more open when operating at low temperatures. If the oil is to be cooled then the oil heat exchanger valve should be cracked open.
11	Open the main water valve to allow for the flow of water. The main valve should be opened slowly and to a maximum of 45° to prevent a rapid and severe pressure drop in other cells. The desired pressure is 30 psi after the water filter.
12	Turn on the sensor switch called "Lambda and Mdot" on the front control panel. Enter the test cell and push the "operate" button on the pressure transducer amplifier so that the LED by the word "operate" is lit.
13	Turn on the dyno controller by pushing the right button on the dyno control panel. Do not press the left button which engages the dyno
14	Turn on the "coolant pump" switch on the front control panel
15	If the oil is to be chilled or circulated then flip the "oil pump" switch on the front control panel and push the start botton on the oil pump controller inside the test cell
16	Using the omega engine controller, set the desired motoring speed. A value of 26.1 corresponds to approximatley 1215 RPM. The motoring speed should be set slighly above the desired testing RPM.
17	Turn on the motor contoller switch on the control panel. The value shown on the omega controller will rise and the motor will make a high pitched sound as it enters overdrive mode.
18	After hearing this sound, briefly crank the engine with the key on the front control panel for no longer than 1 - 2 seconds.
19	If the done correctly the electric motor will start to spin the engine and the engine RPMs as shown on the dyno controller will start to rise and eventually reach a steady value. If the crank time is too short then try a slighly longer crank time, but do not exceed 2 seconds as this will strip the starter.
20	Set the dyno load set point (LSP) to 0. Push the left botton on the dyno contoller to engage the dyno. The engine will briefly slow down but the motor will ramp the speed back up to its initial value.
21	Using the left knob, slowly increase the load until the desired RPM is reached.

Table 2-8: Procedure for engine motoring

Running and firing the engine	
1	After following the engine motoring procedures, increase the LSP so that the engine is running approximately 50 RPM slower than the testing conditions.
2	On the master computer, open the LabView program (Ron_3) and enter "test" into one of the text boxes at the top. Make sure that the fuel pressure is at the desired level. A very low fuel pressure is likely the result of the valves not being set correctly or the accumulator being empty resutling in the piston resting on its stops and being unable to pressurize the fuel lines.
3	Both the slave and master computers should be on. The slave computer needs to be running in DOS mode which can be accomplished by restarting it and selecting "restart in DOS mode". The master computer should use a DOS command prompt.
4	On the slave computer open file "C:\D\single_a" and on the master computer open file "C:\D\master_b".
5	On the master computer enter the operating RPM
6	When prompted on the master computer, enter the target lambda value (usually 1), the injection timing (e.g. 660 CAD aBDC), and the spark timing (e.g. 163 CAD aBDC).
7	On the slave computer enter the desired proportional and integral feedback coeffecients (eg. 0.02 and 0.05) and press enter. Then enter the initial injection duration (1400 - 1900 μsec) and press enter. The duration of the initial duration is a function of MAP and fuel type. The higher the MAP and the higher the percentage of ethanol, the larger the initial duration.
8	The engine sound should change and the engine RPMs should rise assuming good combustion is occuring. This can also be observed by watching the lambda meter readout which should quickly reach the steady value entered into the master computer.
9	If the lambda readout is significnatly (+/- 0.3) from the desired value for more than a few seconds then quickly stop the engine running program with the hardware switch located in the cabin under the desk. The most common reason for these problems is the accumulator being empty or an electrical problem. Use LabView to check the fuel rail pressure and check all electrical connections for any loose plugs.
10	After a failure to achieve good combustion, motor the engine for a few minutes to ensure there is no liquid fuel in the muffler or exhaust lines which can cause a backfire.
11	Using the omega coolant controller set the upper and lower bounds on the coolant temperature. This can be done by pushing the menu button to select and adjust the two set-points. The first set-point is the temperature up to which the coolant heater will run and heat the coolant. The second set point is the temperature at which the solenoid valve will allow cool city water to enter the coolant heat exchanger. These set-points should be set at least 5 degrees apart to prevent rapid oscilation between heating and cooling.
12	The coolant control controller is activated by pressing the enter button until the words "Stby" stop flashing and the contorller enters run mode.
13	LabView should already be open
14	Select view and select "Block Digram." This will show the block diagram of the program. To select a new location for files simply left click the append path block at the far right of the block diagram and select "Browse for new path."
15	The FID and FFID gains can be adjusted by left clicking the DataAnalyst3 block at the far left of the block diagram and selecting "edit".
16	In the front panel of labview the operating parameters for a test can be entered into the corresponding text boxes and those parameters will be combined to make the name under which the file will be saved.

Table 2-9: Procedure for running and firing the engine

Engine shut-down	
1	Flip the hardware switch to end the engine running program which ends the program running on the slave computer and ends the injection of fuel and the firing of the spark plug.
2	The program on the master computer should be ended by entering three zeros (0 0 0). Then the DOS command prompt can be closed.
3	Disengage the dyno by pressing the left button causing the light behind the left button to deactivate
4	Turn off the motor with the switch on the front control panel. The engine should reach zero RPM within a few seconds
5	Turn of the dyno controller by pressing the right button
6	Press "Enter" twice on the coolant controller to put it in stand-by mode.
7	Flip off the motor and coolant heater circuit breakers in the electrical cabinet inside the test
8	The National Instruments chassis and the control panel power supply can be left on.
9	Stop the flow of water by closing the main water supply valve. The other valves can be left in their positions for the next experiment.
10	Ensure that all fuel storage containers are closed and not venting fumes
11	Close the nitrogen tank by turning the top knob clockwise.
12	Drain the nitrogen in the system by turning the regulat knob counter-clockwise.
13	Close all valves (1, 2, 3, 4, 5, 6, 7, 9, 10, 11, and 12) above and below the accumulators, this will ensure that you do not accidentally pressurize the wrong accumulator or introduce the incorrect fuel by accident in the next experiment.

Table 2-10: Procedure for engine shut-down

3 Results

Over the course of the experiments, two baselines were established. The first baseline conditions are highlighted below in Table 3-1.

Engine Speed	**1200 RPM**
MAP	**0.46 - 0.48 bar**
EOI Timing	**120 CAD bTDC**
Spark Timing	**17 CAD bTDC**
Fuel Pressure	**70 bar**
Coolant Inlet Temperature	**60° C**
Fuel	**Chevron Phillips UTG 91**

Table 3-1: Standard conditions for higher load testing

The conditions are set typical of engine operation at medium load and speeds: 1200 RPM and MAP of 0.46 – 0.48 bar. The MAP was set to a high value for the initial tests to study the effect of injecting a substantial amount of fuel into the cylinder. A major issue with GDI engines is that the fuel that enters the cylinder is not initially vaporized. As such, it is of value to observe the engine under high levels of load to emphasize the effect on HC emissions of GDI operation. Under a typical suburban drive cycle the engine would not be at that high of a load for a long period, but it is likely that it would see that level of MAP for brief periods of time when accelerating onto a busy road or at traffic lights.

Due to the nature of the control system, all injection timing is specified in terms of end of injection (EOI) rather than start of injection (SOI). However, the SOI can easily be identified by subtracting the pulse width duration from the EOI. The pulse width duration is a function of the mass of fuel that needs to be injected which is itself a function of level of

loading and the type of fuel. At higher loads more fuel will need to be injected. At the same level of loading, fuel with a lower stoichiometric air-fuel ratio such as ethanol will require a larger injected mass than fuels like gasoline.

The spark timing was found by running a spark sweep on the engine to observe when the maximum GIMEP was observed. Friction and other sources of mechanical inefficiency are almost entirely independent of spark timing. As such, the maximum GIMEP should also correspond to the maximum brake torque (MBT). The results of the spark sweep for gasoline at the higher load is shown in Figure 3-1 below. Although the curve is somewhat irregular, the curve indicates an MBT timing of approximately 17 CAD bTDC.

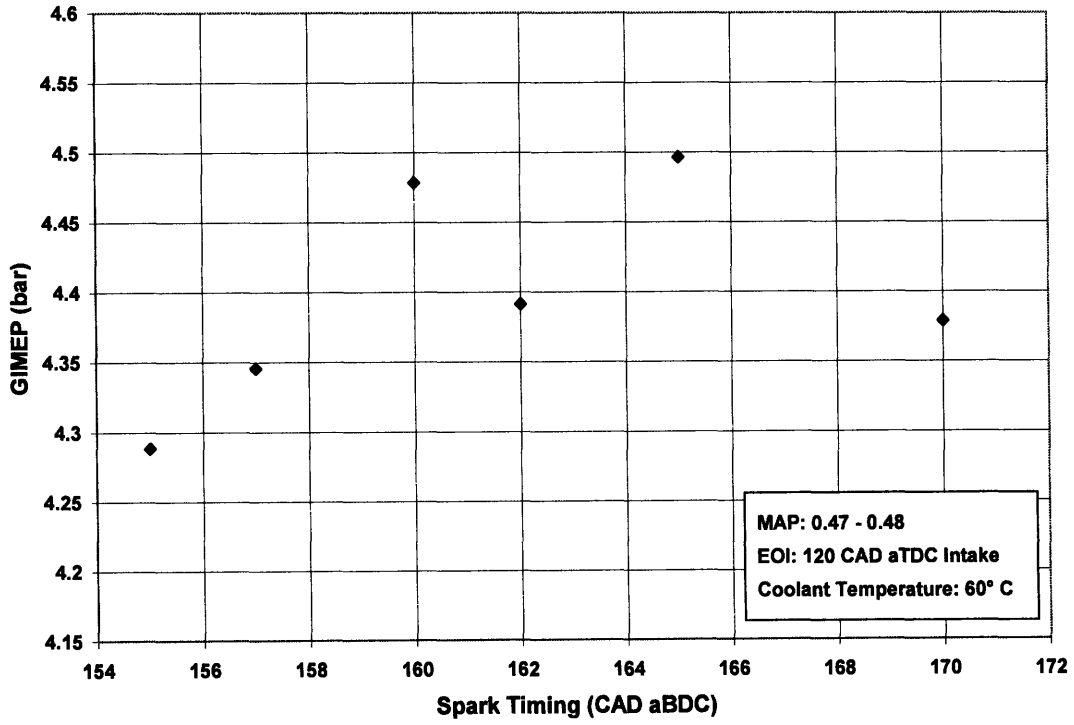

Figure 3-1: Spark sweep for high load condition

The fuel pressure was set at 70 bar because it is the middle of the stock engine operational range which is 40 – 120 bar. In addition, testing of the engine at different fuel

pressure levels showed that a fuel pressure of 70 bar is part of a plateau in HC levels versus fuel pressure when the CMCV is closed, as shown in Figure 3-2.

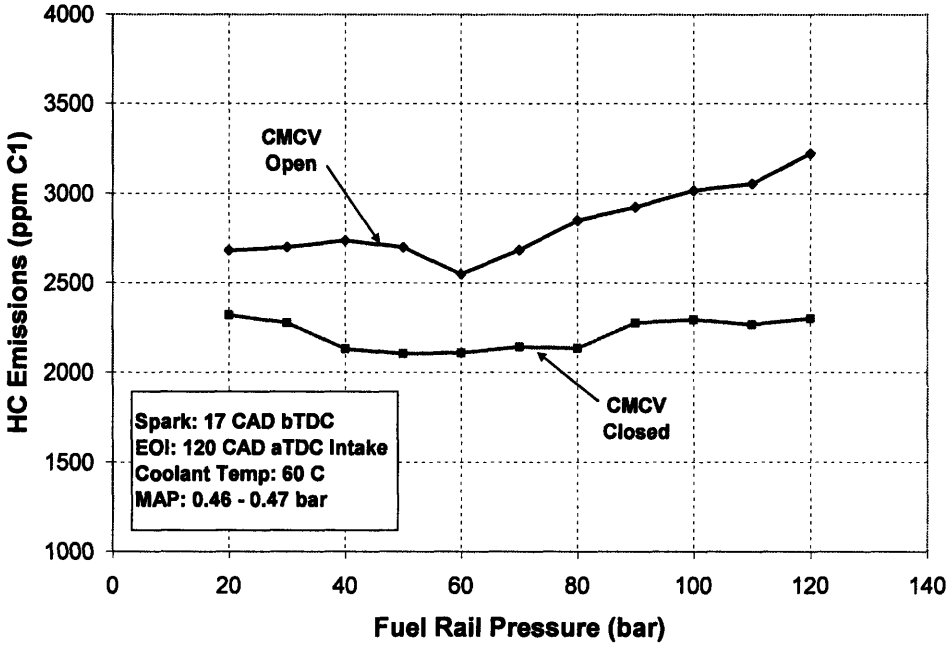

Figure 3-2: HC emissions vs. fuel pressure for UTG 91 with the CMCV open and closed

The coolant temperature of 60° C represents a temperature between an engine at normal ambient temperatures (~20° C) and a fully warmed up engine (~90° C). At this temperature any fuel that contacts an engine surface such as the cylinder walls or piston will substantially evaporate due to the typical thickness of surface films and the vapor pressure of the typical paraffinic components of gasoline as shown in Figure 3-3. Table 3-2 shows the cumulative volume percentage vaporized for UTG 91. For example, if all the components up to C_8 have vaporized, the cumulative volume vaporized would be 83.47%. The selection of UTG 91 as the test fuel was due to it being a standard reference fuel which is frequently used in automotive testing. As such, the results of our experiments can correlated to experiments done in other labs without variances in the composition of the fuel resulting in additional sources of error.

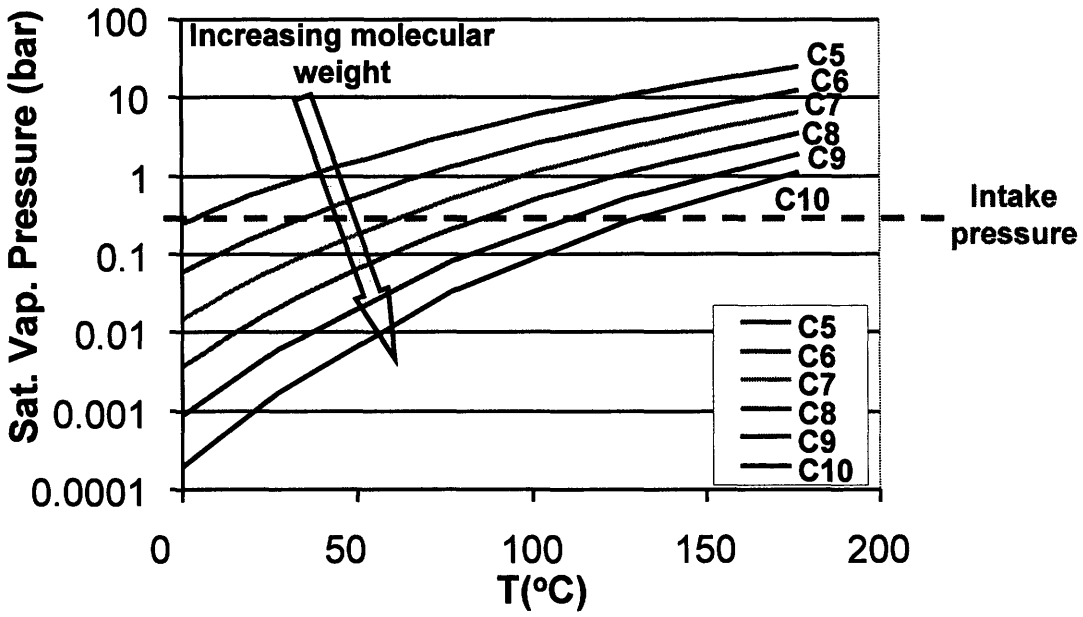

Figure 3-3: Vapor Pressure vs. Temperature for paraffinic hydrocarbons

Carbon Molecules in Heaviest Species Vaporized	Cumulative Volume % Vaporized
C5	19.14
C6	29.02
C7	52.40
C8	83.44

Table 3-2: Volume percentage vaporized based upon heaviest vaporized species for UTG 91

Later, a different baseline conditions was established with were set which were more like those that would be seen in an engine at fast idle. The coolant temperature is still slightly above that which would be seen when the engine first starts, but is close to the temperature that would be seen if the engine was allowed to warm up for a few minutes. The conditions are highlighted below.

Engine Speed	**1200 RPM**
MAP	**0.27 bar**
EOI Timing	**120 CAD bTDC**
Spark Timing	**17 CAD bTDC**
Fuel Pressure	**70 bar**
Coolant Inlet Temperature	**40° C**
Fuel	**CP UTG 91, 100% Ethanol**

Table 3-3: Standard conditions for fast idle testing

The MAP of 0.27 bar is more representative of the loading that would be seen under a fast idle or light load condition. The engine speed was kept the same. Another spark sweep was performed on E85 to see if it had similar spark timing. The resulting spark sweep is shown below in Figure 3-4. The MBT spark timing was found to be closer to 20 CAD bTDC. Since the optimal spark timings were close for both fuel types, if was decided to keep the spark timing at 17 CAD bTDC to minimize the variables.

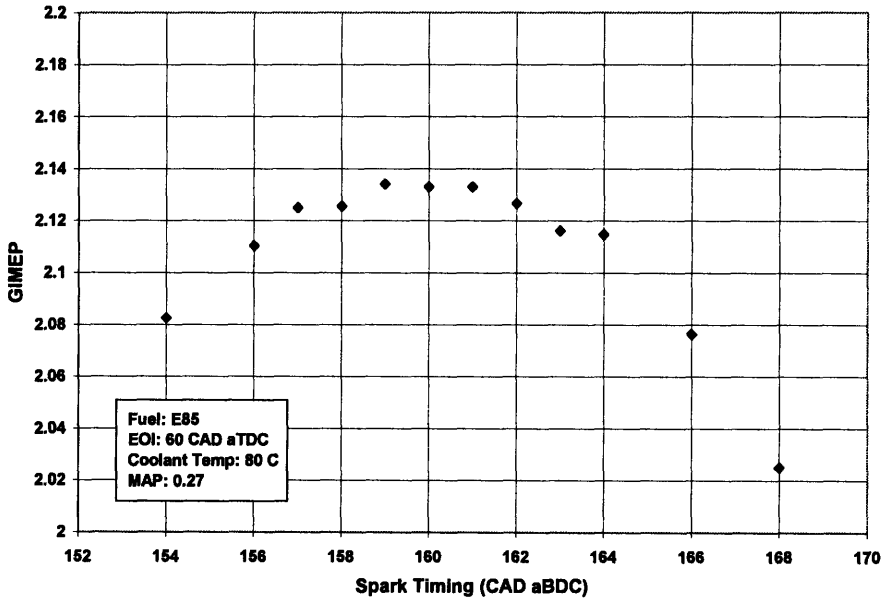

Figure 3-4: GIMEP vs. Spark Timing for mixture of 85% ethanol and 15% UTG 91 by volume

Under both cases, the baseline operating conditions were not always held constant. Instead, the baseline simply established the values that would be used when varying other variables. For example, when doing a spark sweep for an ethanol blend, the coolant temperature would be set to 40° C, fuel pressure would equal 70 bar, and the EOI would be set to 60 CAD aTDC. For EOI sweeps, multiple temperatures were used in order to understand the effect of temperature under a variety of conditions. For the majority of these tests three different temperatures were used: 20°, 40°, and 80° C.

Due to the nature of the set-up it was not possible to perfectly maintain the MAP. As such, for the tests at low load, the throttle was set so as to make the MAP close to 0.27. Then, over the course of all subsequent tests, the throttle was not touched and the MAP varied by +/- 0.015.

As shown in the diagram for the fuel system, a large number of valves and a long length of piping separate the high pressure gas bottle from hydraulic accumulator and the accumulator from the actual fuel rail. As such, there is a noticeable pressure loss from the regulator to the fuel rail. In addition, the internal friction between the piston and the cylinder in the accumulator results in a pressure loss. Together these two factors result in the regulator pressure having to be set above the desired fuel pressure. Since the pressure regulator uses a fairly simple mechanism to control gas pressure, it is hard to predictably and reliably set the fuel rail pressure. The net result is that the fuel pressure will sometimes be +/- 1.5 bar from its desired value. However, this only represents a 2% error and given the flat response of HC to fuel pressure, should not result in significant error.

The coolant system has a built in lag to changes in temperature because the heating element and the heat exchanger both act in or before the mixing tank. As a result, it takes

some time for changes in coolant temperature to reach the coolant temperature sensor located where the coolant enters the engine. As a result, the coolant temperature can, over a series of experiments, vary by +2/-4 C. However, the actual parameters that influence combustion are the temperatures of the engine and piston which both have a large thermal mass. As such, although the coolant temperature may vary, the average cylinder and piston temperature over the course of the experiment is constant.

Originally tests were done with only 50 cycles being recorded due to limits on the ability to analyze large data sets. A given set of conditions would be tested four times and averaged. However, it was found that 50 cycles was not sufficient for the effect of a single errant cycle to be averaged out and for variability calculations to be reliable performed. As such, the testing procedure and analysis was adjusted and 300 cycles were recorded for a given set of parameters.

This increase in cycles recorded did not allow for multiple tests to be done for every data point. As such, when an EOI sweep was performed, the EOI would be set randomly rather than sequentially. Any tendency for a given data point to be influenced by the previous test would become obvious because the data point would not conform to the points before and after that point. Any points that were found to be anomalies were retested and averaged or tests were performed on EOI timings intermediate to the conflicting values. For example, if a test at an EOI of 120 did not fit with the tests done at 110 and 130, then an EOI of 120 would be retested, or an EOI of 115 and an EOI of 125 would be tested. Sometimes all three tests were done to ensure reliable data.

3.1 Coolant Temperature Variations

A study was done to understand the effects of the coolant temperature on the HC emissions. The coolant temperature was varied between 20° – 90° C. The experiment was performed both with the charge motion control valve closed and open. In addition, the fuel isopentane was used since it has a boiling point of 28° C [10]. Since the engine cylinders and piston operate at a temperature above that of the coolant, under all coolant temperature tested, the isopentane should immediately vaporize after injection and there should be no effect due to surface impingement.

In general it was expected that the HC emissions would steadily decrease as the coolant temperature and engine temperature was increased. The different reasons for this expectation are provided by Cheng et. al. [1] and are summarized and explained in the table below.

Mechanism	Explanation
Crevices	Ideal Gas law results in less mass in the same volume at higher temperatures
Deposits	Ideal Gas Law
Oil Layer	Henry's Law states that solubility decreases as temperature increases
Liquid Fuel	Higher surface temperatures result in more species boiling on contact and faster boiling

Table 3-4: Mechanisms relating coolant temperature to HC emissions

The plot of HC emissions vs. coolant temperature is shown below. In general, all three series show the same decreasing level of HC emission with increases in temperature. Under all three conditions the HC emissions decrease until the coolant temperature reaches

40° C. Both the UTG 91 (closed) and the isopentane (open) demonstrate a consistent and almost linear decrease in HC emissions as the coolant temperature increases above 40° C. The open valve case for UTG 91 flattens from 40° to – 60° C. It is not clear why the flattening occurs.

It is interesting to note that the slope of the isopentane curve is less than that for UTG 91. One possible reason for the difference may be due to the fact that gasoline is a composite of many different organic compounds each with a different boiling point. As a result, gasoline will continuously experience a benefit from an increase in surface temperature, while isopentane which flash boils as soon as it is injected does not have this benefit with increasing engine temperature. The absolute value of the HC, however, also depends on the oxidation process.

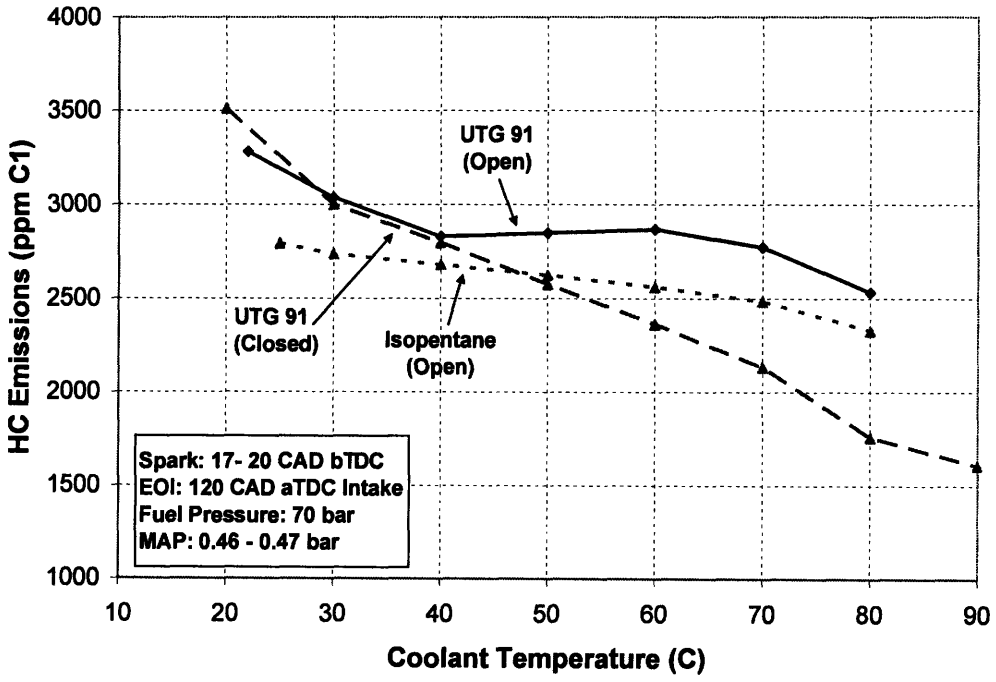

Figure 3-5: HC emissions for UTG 91 and isopentane as a function of coolant temperature

3.2 *Injection Timing at High Load*

A thorough sweep of different injection timings was done. The sweeps were done with both UTG 91 and isopentane. In addition, tests were done with both fuels with the CMCV open and closed. The resulting HC levels are shown in Figure 3-6 below. The similarity of the two sweeps with isopentane shows that there is little effect on mixing for fuels which are already vaporized. Instead, the effect of the CMCV might be to redirect the flow in such a way as to reduce impingement on cooler surfaces or increase the rate of vaporization through increased mixing. The two plots for UTG 91 show very similar trends. At highly advanced injection timings the two curves have almost exactly the same shape and value. However, as the injection timing is retarded, the plot in which the CMCV is closed falls at a faster rate. This might be the effect of the redirection of the flow which has a larger effect when there is more room and time for the swirling motion to have an effect.

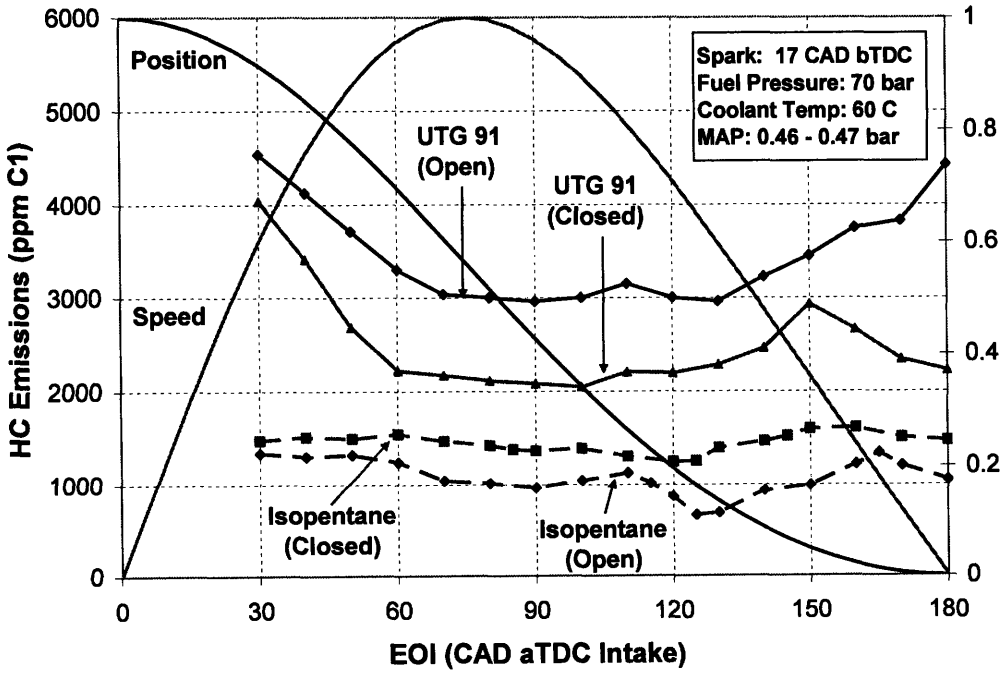

Figure 3-6: HC emissions and piston speed and position for UTG 91 and isopentane

In order to better understand the mixing phenomenon within the cylinders, the average level of carbon-monoxide was measured from the exhaust stream. In is important to remember that these readings are averaged, are sampled 180 cm from the exhaust valve and have passed through the ice-bath condenser. As such, a significant amount of post stream oxygenation can occur. The carbon monoxide and HC levels are shown for tests at two different temperatures in Figure 3-7.

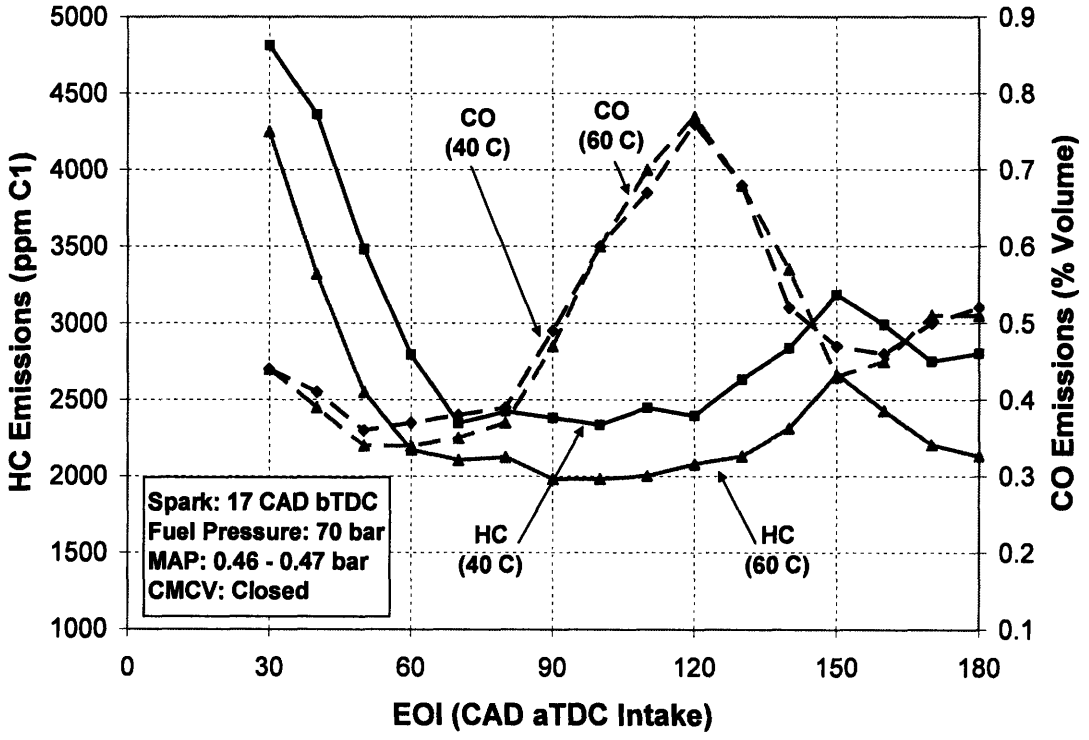

Figure 3-7: HC and CO emissions vs. fuel injection timing for a coolant temperature of 40° and 60° C

Several observations can be made from the data. First is that the carbon monoxide levels are all under 1% which is an appropriate value for stoichiometric combustion. As such, the fuel-air ratio is being well controlled and the fuel to air ratio is being maintained correctly at a lambda near 1. Secondly, it is clear that the CO levels are not proportional to HC levels. Although the high carbon monoxide levels at very early injection timings correspond to high

HC levels, the rise in HC levels which peaks at 120 CAD aTDC Intake does not correspond to rise in HC levels. In fact, after the peak in CO levels, the HC levels begin to rapidly rise as the CO levels rapidly fall. The third observation is that there is a dramatic rise in CO levels which occurs near an EOI timing of 120 CAD aTDC Intake. The shape and timing of this peak is not affected by coolant temperature; and, as later tests will show, is neither a function of fuel loading nor fuel type.

3.3 Sweep of End of Injection at Low Load

Tests under conditions more representative of fast idle conditions were performed. The results are shown below in Figure 3-8. It can be seen that the shape of the CO curve is almost exactly the same as that under higher loading. The peak in the CO curve has become advanced by 10 degrees to an EOI of 110 CAD aTDC Intake. In addition, the magnitude of the CO peak has decreased from 0.76 % to 0.65%. However, neither of these is a major change and thus supports the claim that the CO signature is almost entirely independent of loading and temperature.

The shape of the average HC emissions vs. EOI is also very similar to those under higher loading. Both sets of tests show high HC emissions at highly advanced injection timings, which decrease as the injection timing is retarded. In both cases, the HC signature flattens out until the EOI reaches a value of approximately 120 CAD aTDC Intake. The HC level of the emissions then begins to rise until reaching a peak around 150 CAD aTDC Intake and then slowly declines.

The role of loading can also be noted from the two charts. The minimum HC levels are 2500 ppm C1 for the higher loading at 40° C and 1500 ppm C1 for the lower loading at 33° C. The rise in HC levels that occurs as the timing is advanced seems to almost linearly depend on

the level of loading. The HC levels rise by approximately 2500 ppm C1 at high load and 1500 ppm for the lower load. However, the rise in HC levels that occurs during the peak centered at an EOI of 150 CAD seems to be independent of loading in that the HC levels rise by 750 ppm C1 for both the high and the low loads.

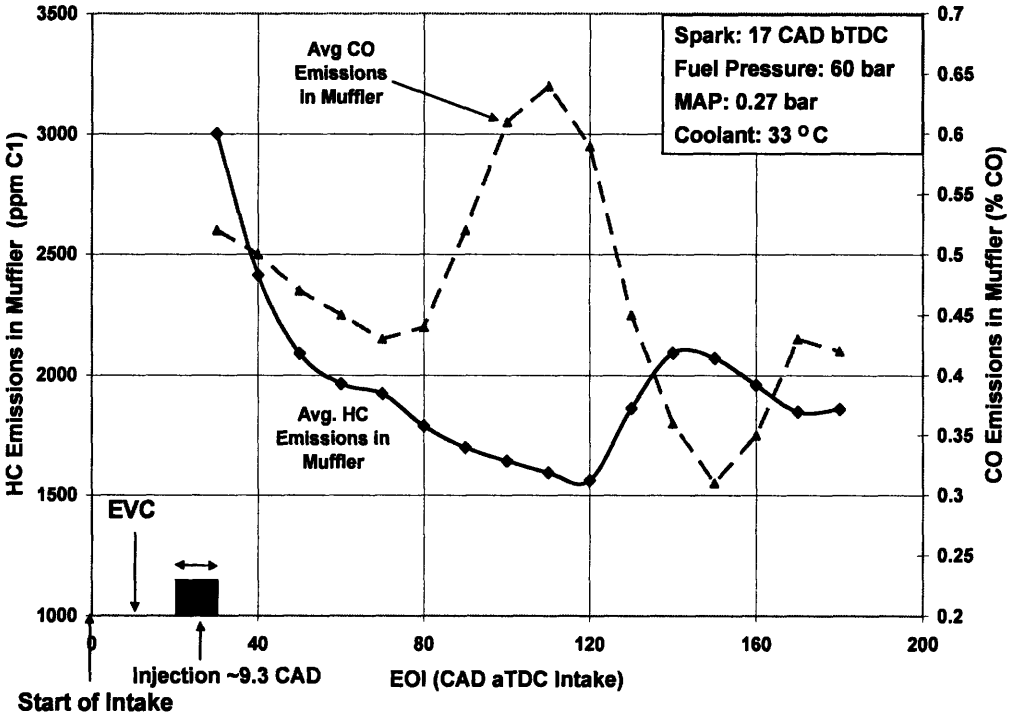

Figure 3-8: HC and CO emissions for UTG 91 at low load

3.4 Injection Timing Sweep of Ethanol Blends and UTG 91

With the greater introduction of ethanol into automotive gasoline, it is important to understand the effect on emission and fuel conversion efficiency for these different fuels. As such, tests were performed on fuels composed of 15, 40, and 85% ethanol by mass. Tests were also performed on gasoline under the same conditions to provide a baseline. It should be noted that the seals in the FFID were resealed between the previous set of tests and these tests and several internal offsets were fixed. As such, the magnitude of the HC emission is higher

for gasoline under the same test conditions. However, observation of the 33° C tests from Figure 3-8 and the 40° C test from Figure 3-9 shows that the plot has simply been shifted up by approximately 1500 ppm C1 and that the shape and magnitude of the variances in HC emissions are almost exactly the same. It is also important to note that the FFID has a different sensitivity to oxygenated fuels and thus the measured HC emissions for ethanol blends is less than the actual HC emissions. The error in measured HC levels increases as the proportion of ethanol in the fuel is increased.

3.4.1 Average Hydrocarbon Emissions

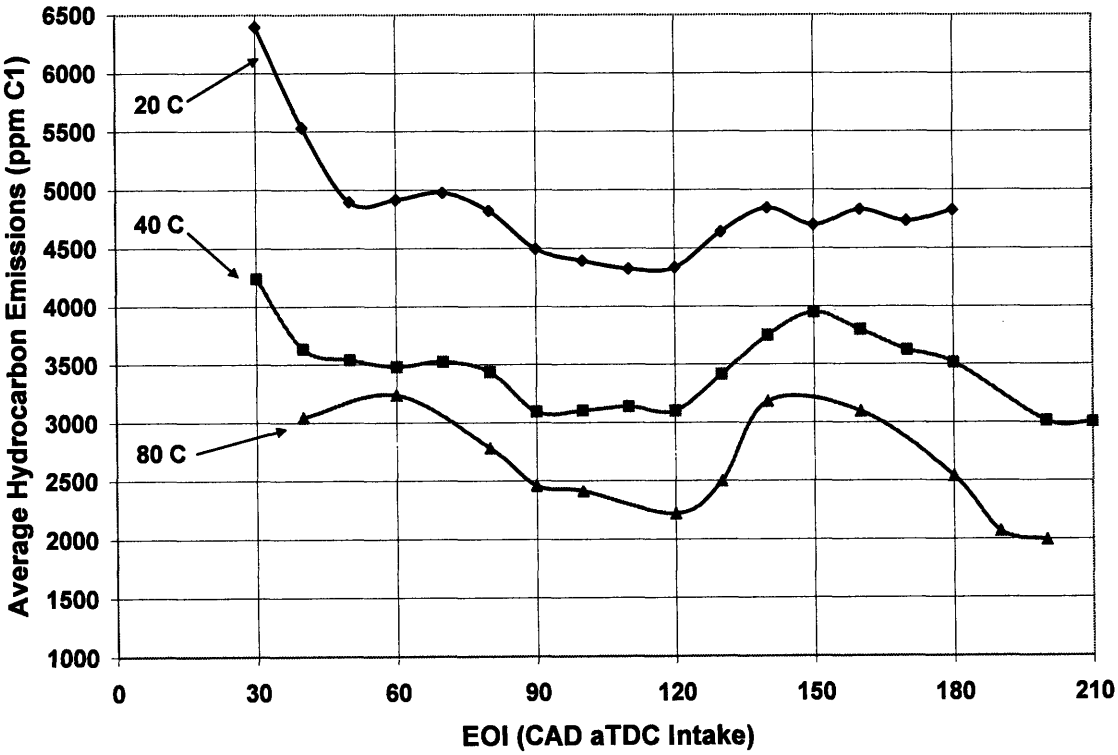

Figure 3-9: Hydrocarbon emissions for UTG 91

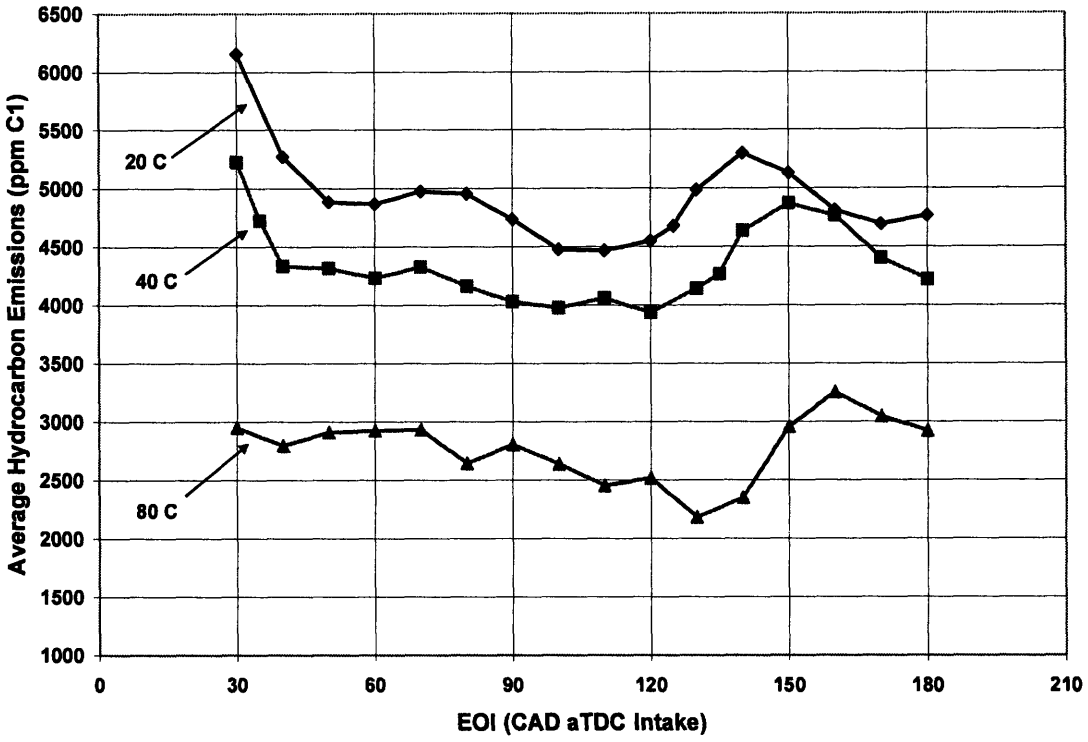

Figure 3-10: Average Hydrocarbon emissions for a 15% ethanol, 85% UTG 91 blend by mass

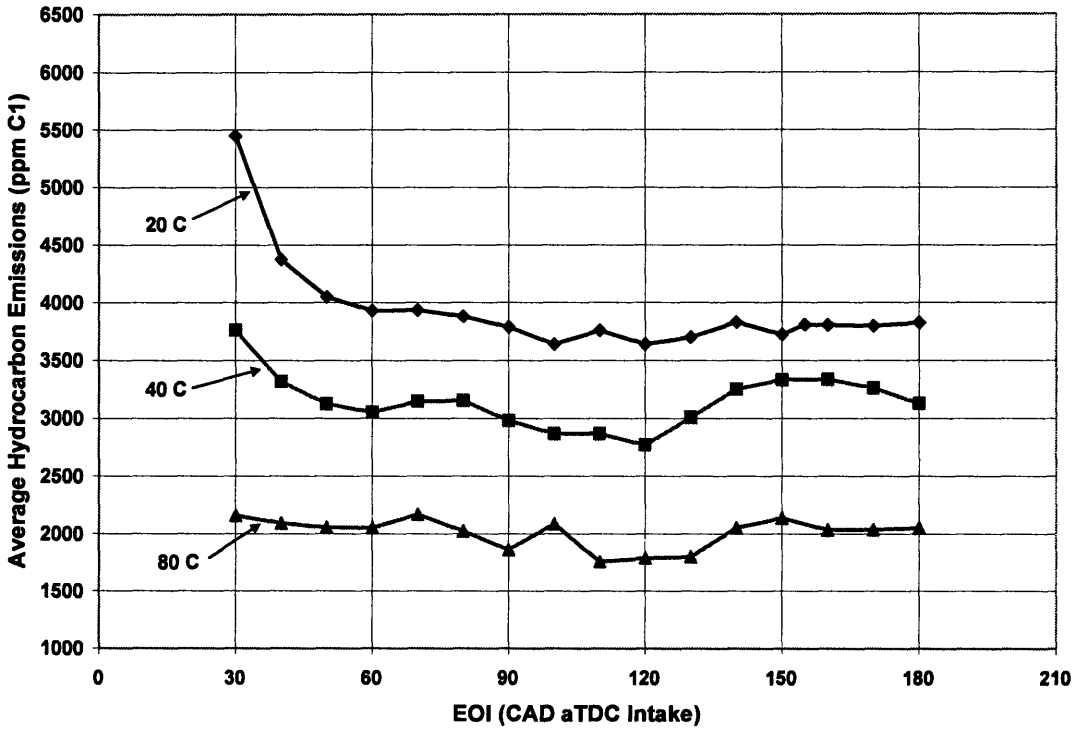

Figure 3-11: Average hydrocarbon emissions for a 40% ethanol, 60% UTG 91 blend by mass

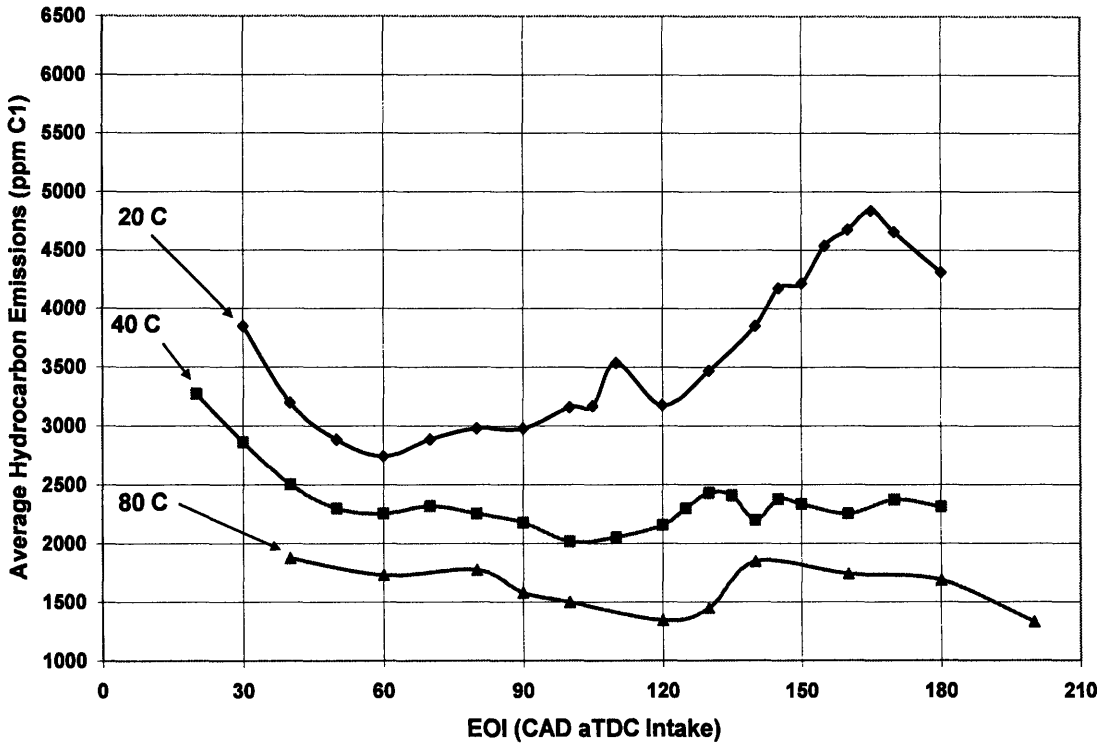

Figure 3-12: Average Hydrocarbon emissions for a 85% ethanol, 15% UTG 91 blend my mass

3.4.2 Indicated Fuel Conversion Efficiency

The GIMEP, fuel rail pressure, and pulse duration were used along with the injector calibration curves to calculate the indicated fuel conversion efficiency under different conditions. The general trend is for the efficiency to decrease as the injection timing is retarded until reaching a minimum value near 120 CAD aTDC. A hypothesis about what might be causing this behavior is that fuel is being lost due to contact with the colder liner surfaces.

It takes a certain amount of time for the fuel to travel across the cylinder and come in contact with surfaces such as the piston or cylinder wall. Since gasoline in general and UTG 91 in particular is composed of many different compounds, each with its own bubbling point, it is possible for a fuel to come in contact with a surface which is not hot enough to

completely vaporize the fuel before it becomes captured by the upward piston motion. Earlier the injection timing allows the fuel more time to vaporize before the piston can entrain the fuel. In addition, an earlier injection results in the fuel contacting higher on the cylinder walls where the temperature is higher resulting in a faster rate of vaporization.

The velocity of the piston also plays a role. When the piston is moving fast, the air flowing past the injector will also move quickly. The result is that the fuel is less likely to directly contact a surface and puddle; instead, it will be more evenly dispersed over the cylinder and piston. The interaction of the fuel spray with the charge motion and the resulting mixing process would affect the emissions and the amount of fuel available for combustion.

When considering all these separate factors together it, it is possible that for UTG 91 and ethanol blends containing a high proportion of gasoline, an injection timing of 120 CAD aTDC intake results in the fuel coming in contact with colder sections of the cylinder wall where the fuel does not have time to vaporize quickly enough to avoid being entrapped in the piston rings or the oil. The 85% ethanol blend does not have this problem to as high a degree because this blend almost completely vaporizes within a narrow band of temperatures as shown in Appendices 6 and ethanol has a vapor pressure equal to 0.27 bar when it reaches a temperature of approximately 47° C as shown in Appendices 7. As such, as long as the majority of the cylinder walls are above that temperature, the fuel will completely vaporize before it can become trapped in the piston rings or oil. However, once the majority of the engine is below the vaporization temperature, the fuel will not be able to vaporize until the air temperature increases during the compression stroke. The result would be the steady decrease in efficiency shown in Figure 3-16.

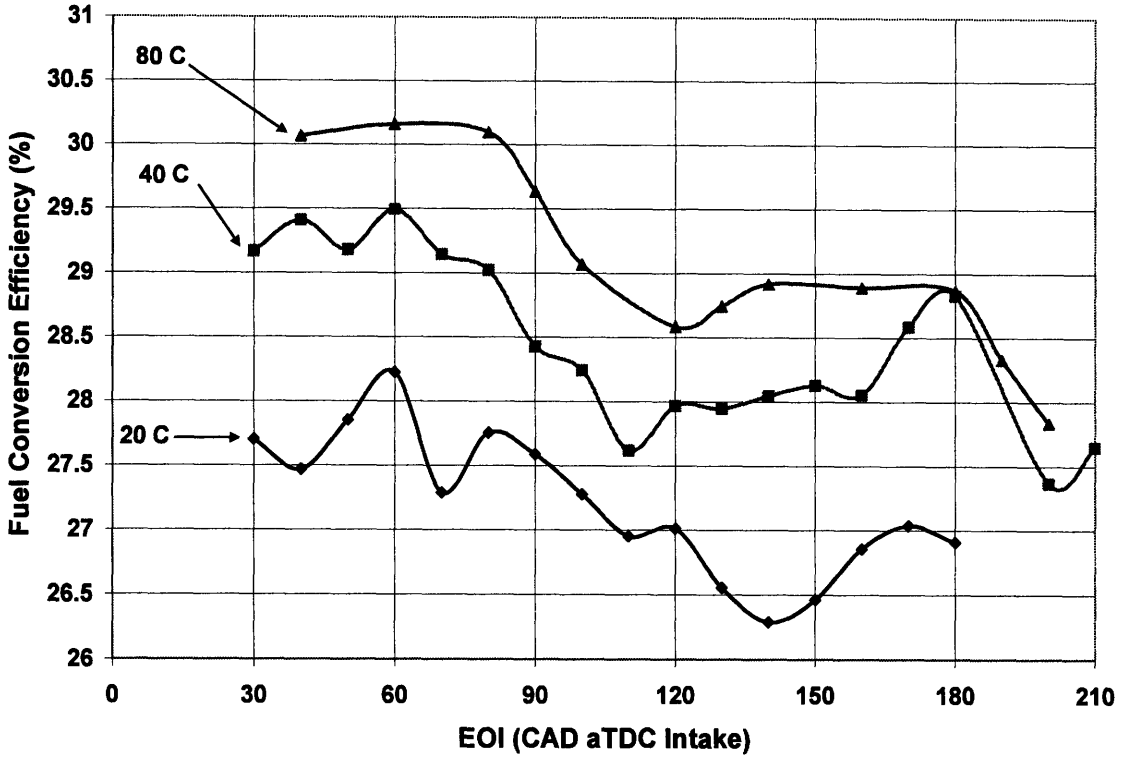

Figure 3-13: Gross indicated fuel conversion efficiency for UTG 91

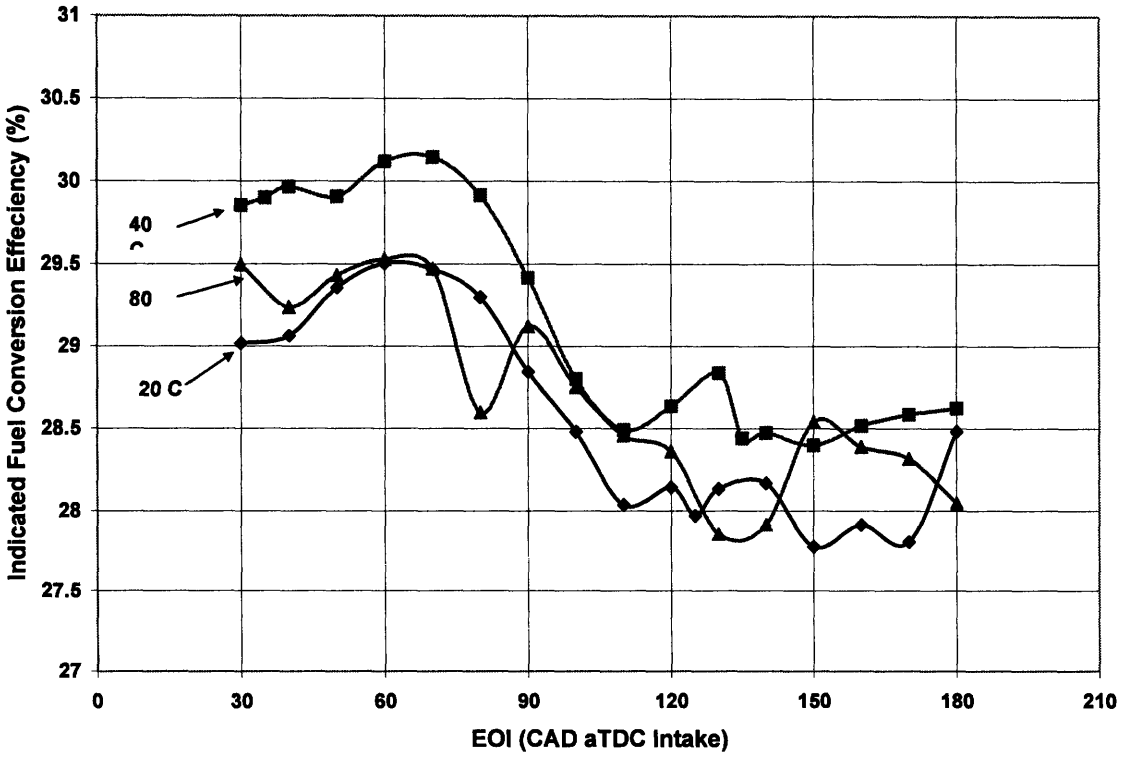

Figure 3-14: Gross indicated fuel conversion efficiency for 15% ethanol and 85% UTG 91 by mass

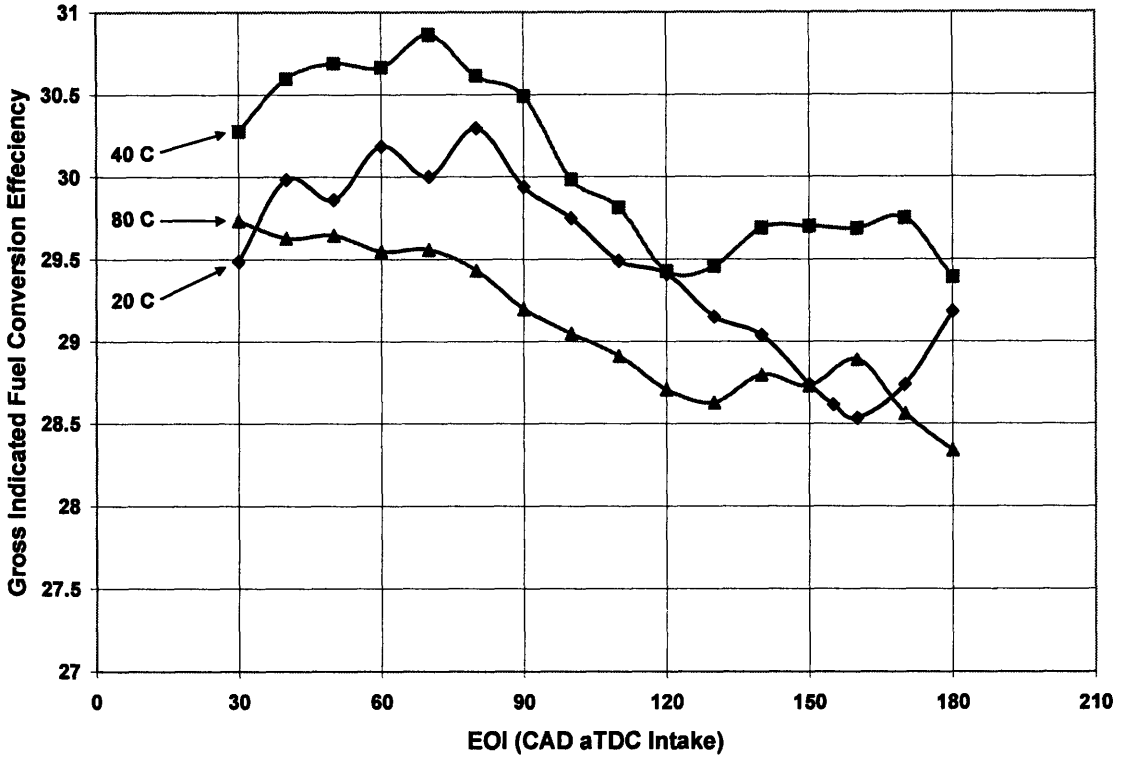

Figure 3-15: Gross Indicated fuel conversion efficiency for 40% ethanol and 60% UTG 91 by mass

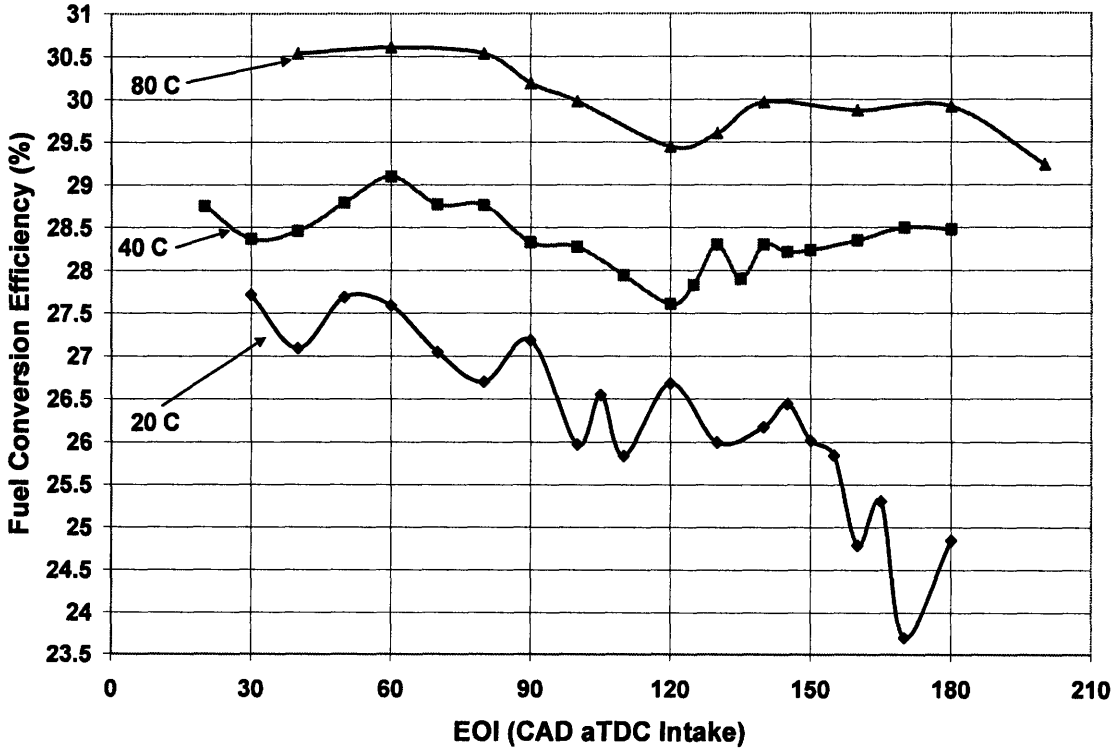

Figure 3-16: Gross indicated fuel conversion efficiency for 85% ethanol and 15% UTG 91 by mass

3.5 *Instantaneous HC emissions near the exhaust port*

The HC emissions sampled 15 cm from the exhaust port were averaged on a crank degree basis for all 300 cycles. The resulting plots of HC levels vs. CAD were then compared for early an EOI of 30, 120, and 180 CAD aTDC. In all three cases the curve shows a very similar shape. There was some concern that for early injection timings, there might be a direct flow of fuel from the injector into the exhaust valve. However, the instantaneous HC emissions for an EOI of 30 CAD aTDC does not show any rapid rise in HC levels at EVO due to the blow out of the hydrocarbons accumulated near the exhaust valve.

3.5.1 HC emissions for Gasoline

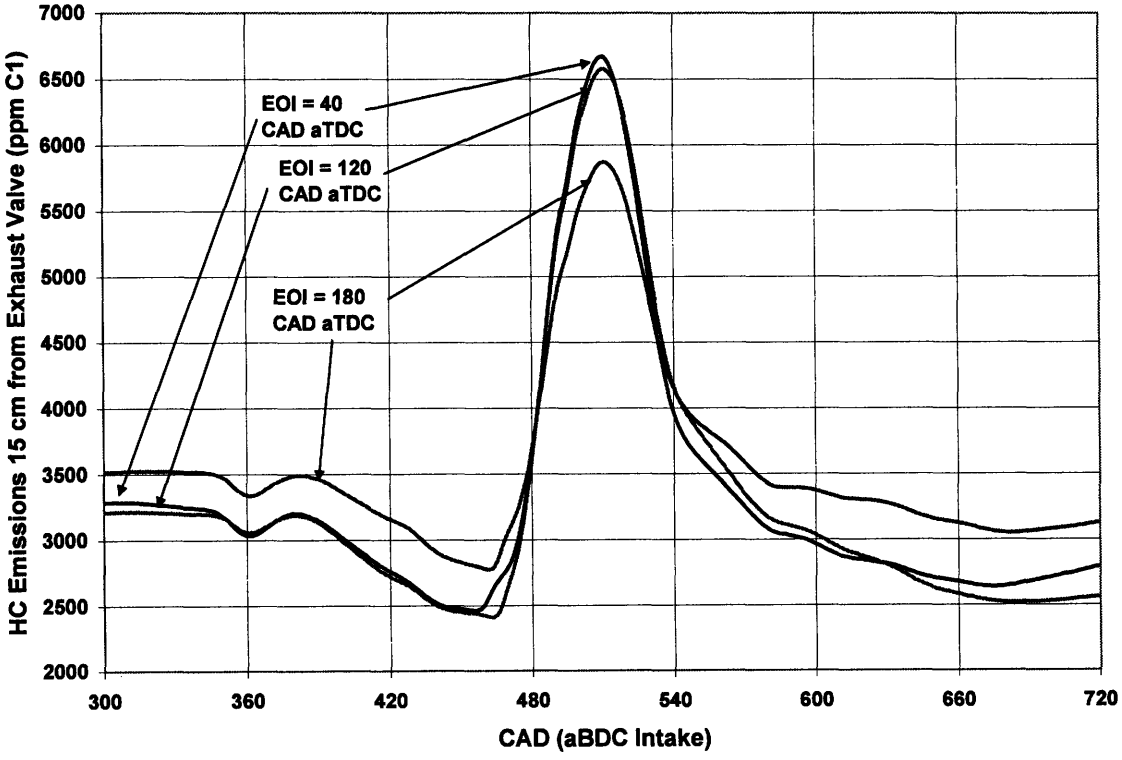

Figure 3-17: HC emissions vs. CAD for UTG 91 with coolant at 20° C

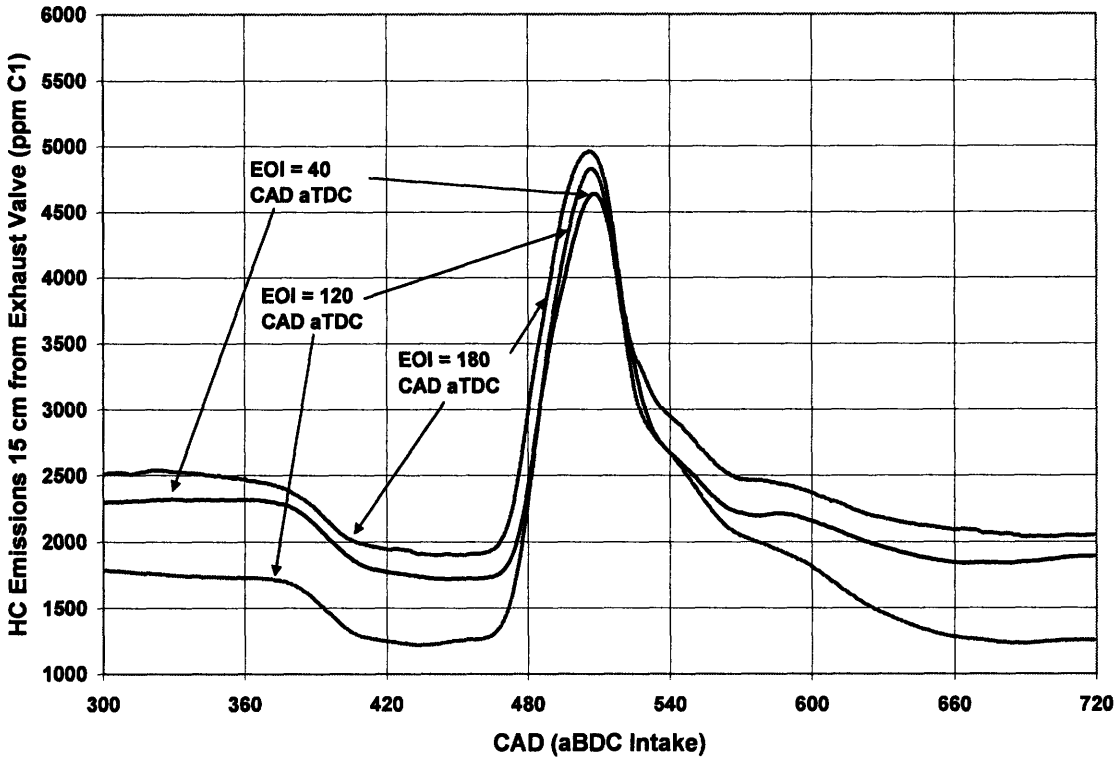

Figure 3-18: HC emissions vs. CAD for an E85 with coolant at 40° C

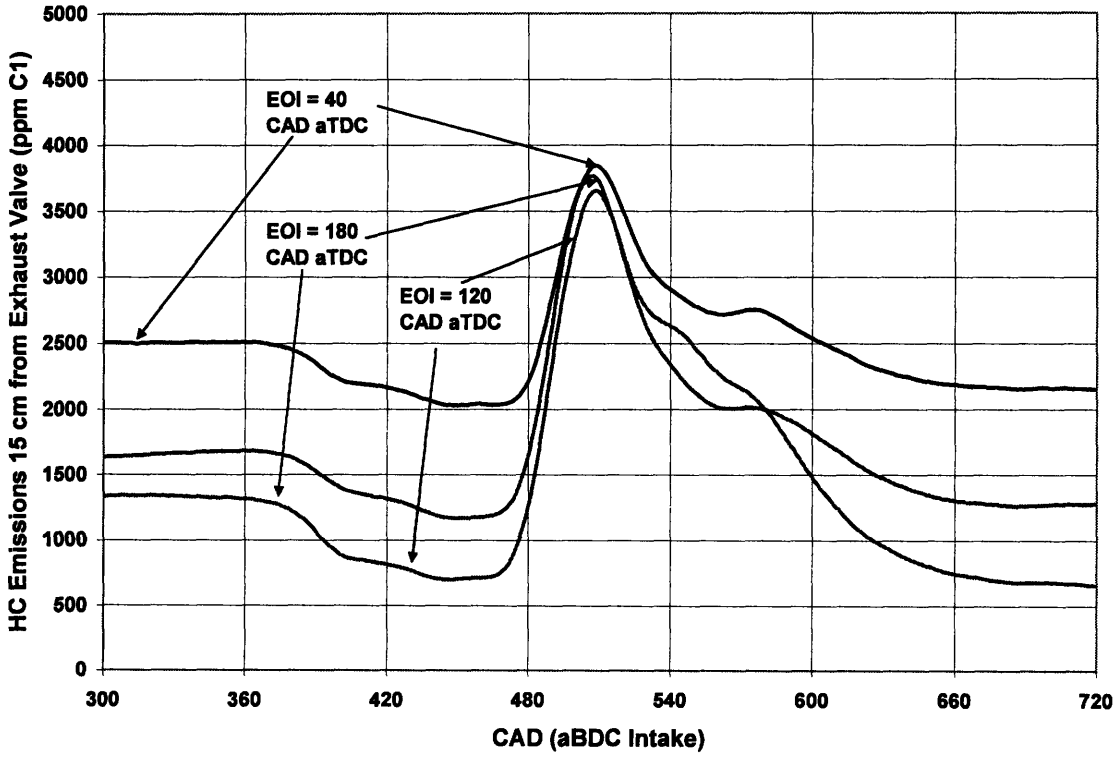

Figure 3-19: HC emissions vs. CAD for an E85 with coolant at 80° C

3.5.2 HC Emission for 85% Ethanol and 15% UTG 91 by mass fuel blend

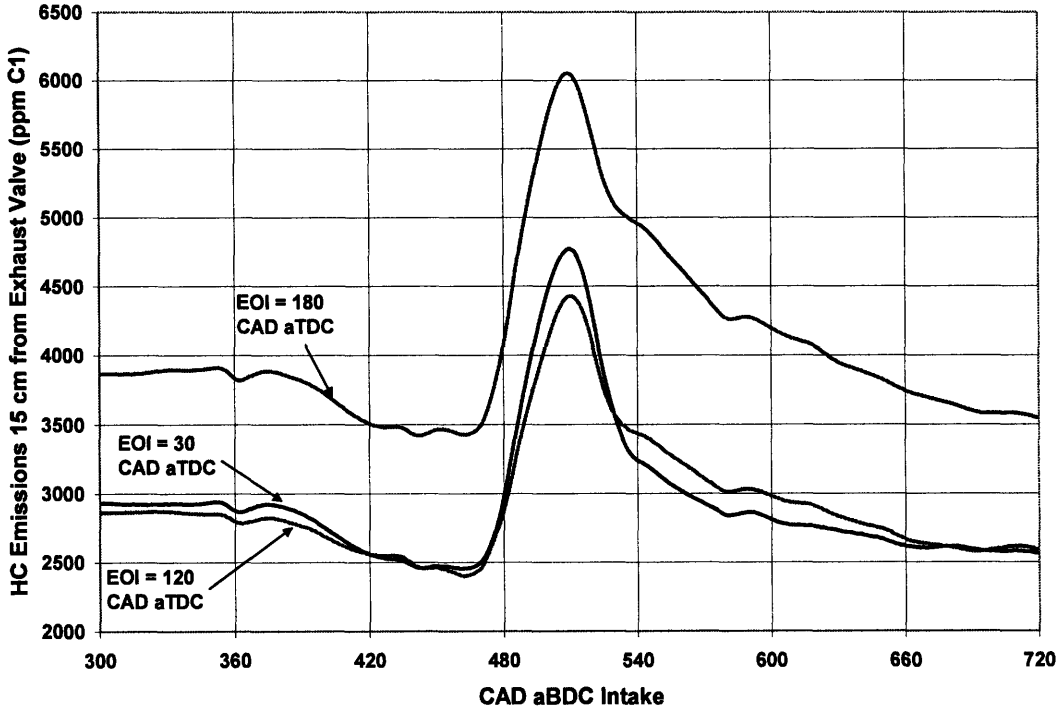

Figure 3-20: HC emissions vs. CAD for an E85 with coolant at 20° C

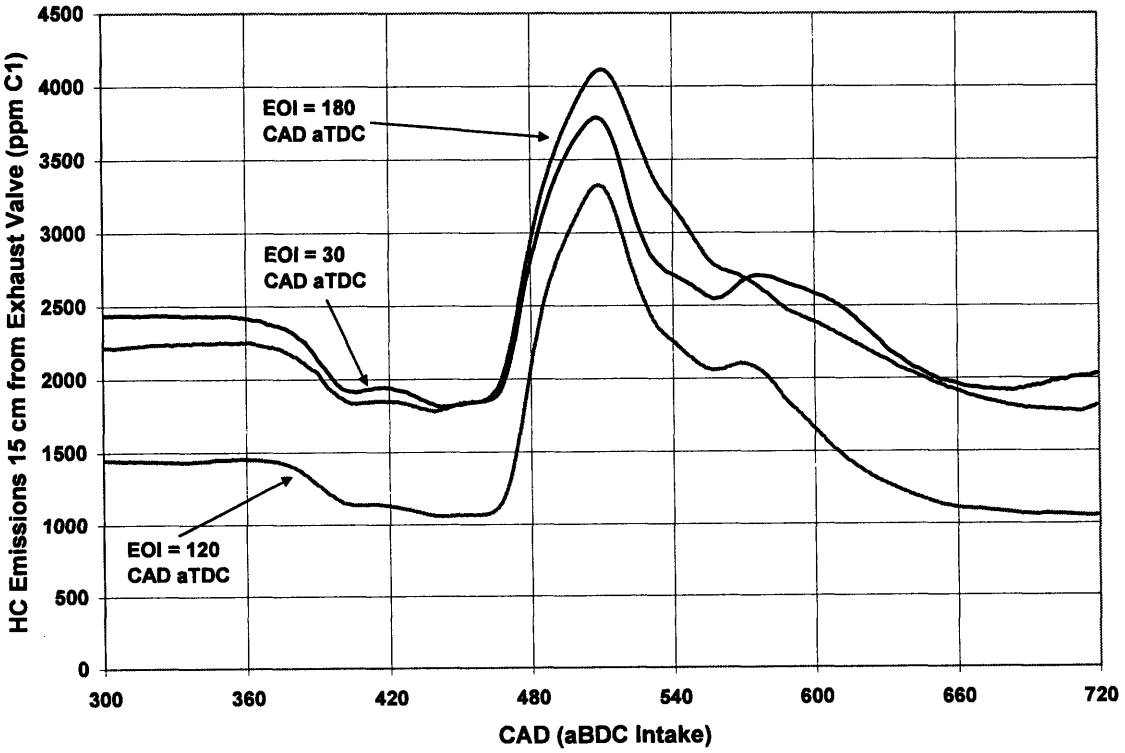

Figure 3-21: HC emissions vs. CAD for an E85 with coolant at 40° C

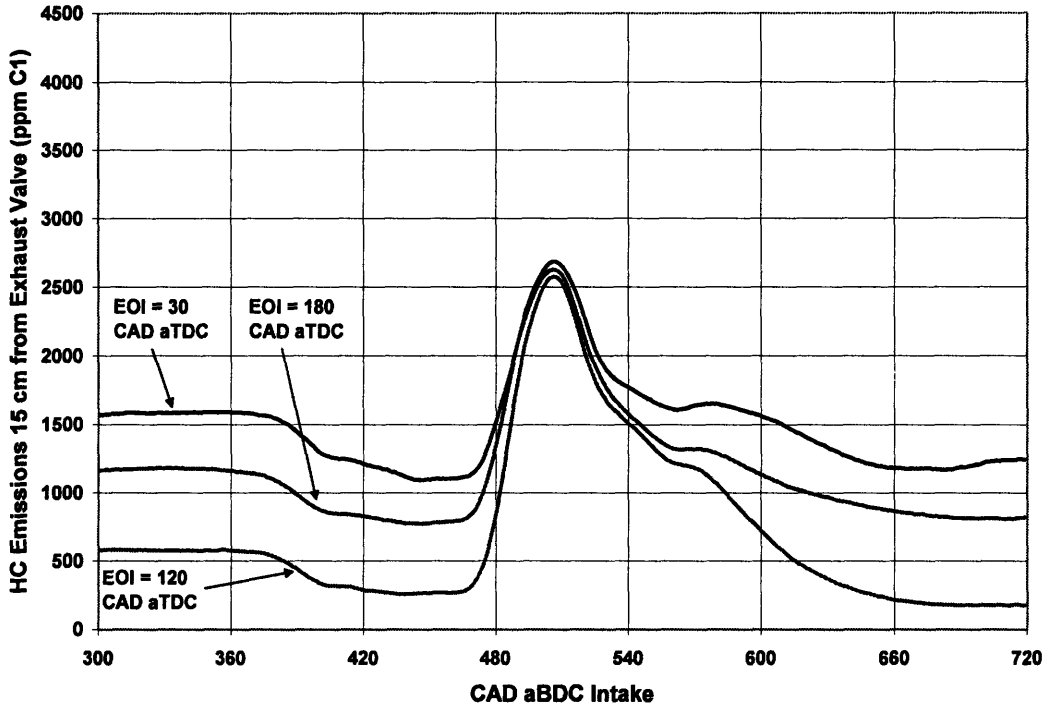

Figure 3-22: HC emissions vs. CAD for an E85 with coolant at 80° C

3.6 In Cylinder Pressure for Different Injection Timings

The plots of cylinder pressure as a function of crank position provide useful information about the combustion event. Under all coolant temperatures and injection timings, the general shape of the plots is the same. There is a steady rise in pressure due to compression. Then at approximately 165 CAD aBDC Intake, the cylinder pressure quickly rises as the combustion front moves through the cylinder. The peak pressure is achieved at 15 – 20 CAD aTDC which corresponds to MBT timing. The cylinder pressure then begins to fall during the expansion stroke. The smoothness of the pressure signal indicates that no knock occurred within the cylinder.

The pressure signal also suggests another possible explanation for trends observed in gross indicated fuel conversion efficiency. In almost every test the peak pressure is highest for the earliest injection timing. Since the indicated power output is the area under the

pressure vs. volume curve, a higher peak pressure and higher pressure plot following the peak pressure will result in a higher power output. If the mass of fuel injected is approximately the same for all tests, then this higher power output will translate to a higher indicated fuel conversion efficiency.

For gasoline it is not clear what is accounting for this higher peak pressure. The pressure plot prior to the start of combustion is almost the same for all three injection timings. As such, the higher peak pressure can only be accounted for by the cylinder gasses having a higher internal energy for the earlier injection than for later injection timings. If the magnitude of heat transfer into the cylinder gasses from the piston and cylinder walls during the combustion event is assumed to be approximately equal for all injection timings then the additional thermal energy must come from the combustion of the fuel. As such, a lower peak pressure could be the result of fuel loss due to impingement of fuel on the piston or cylinder walls and a loss of fuel to the piston rings or lubricating oil.

In the case of the 85% ethanol blend, the earlier injection timing shows a higher pressure prior to combustion. This could be due to the higher heat of vaporization of ethanol (840 kJ/kg) when compared to gasoline (305 kJ/kg). This means that it takes significant additional thermal energy to vaporize ethanol when compared to gasoline. When the fuel is injected earlier, the cylinder and piston can provide this thermal energy, resulting in a higher thermal energy for the cylinder gasses. When the charge is injected later, the thermal energy must come from the air charge, resulting in a lower thermal energy for the charge, which due to the charge mass being constant, results in a lower initial pressure. The higher initial pressure for the earlier injection timing results in a higher pressure prior to combustion and a higher pressure during combustion. As the coolant temperature increases, the time required to

completely vaporize the ethanol decreases and the effect of cylinder pressure of injection timing decreases. The pressure plot then becomes dependent on the efficiency of combustion and the loss of fuel, both of which are impacted by piston position and spray impingement.

3.6.1 UTG 91

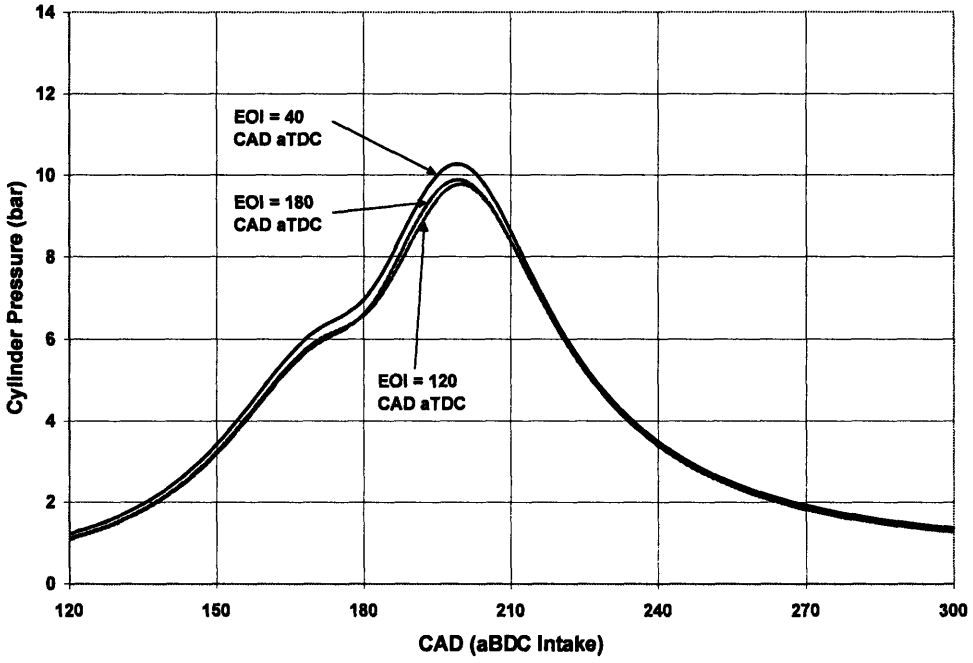

Figure 3-23: Cylinder Pressure for UTG 91 for coolant temperature of 20° C

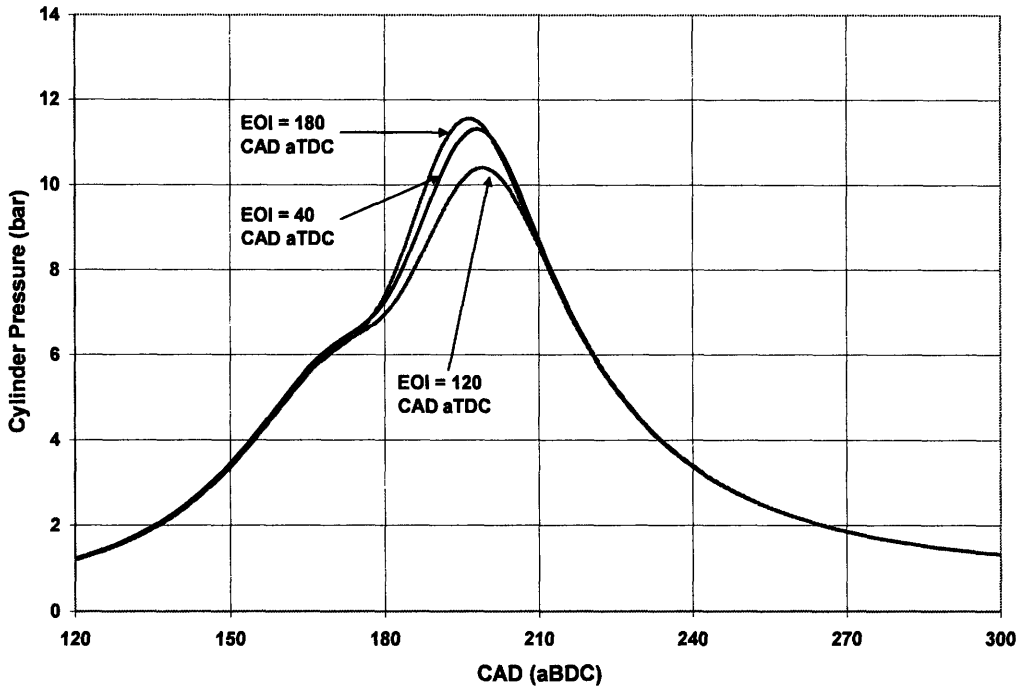

Figure 3-24: Cylinder Pressure for UTG 91 for coolant temperature of 40° C

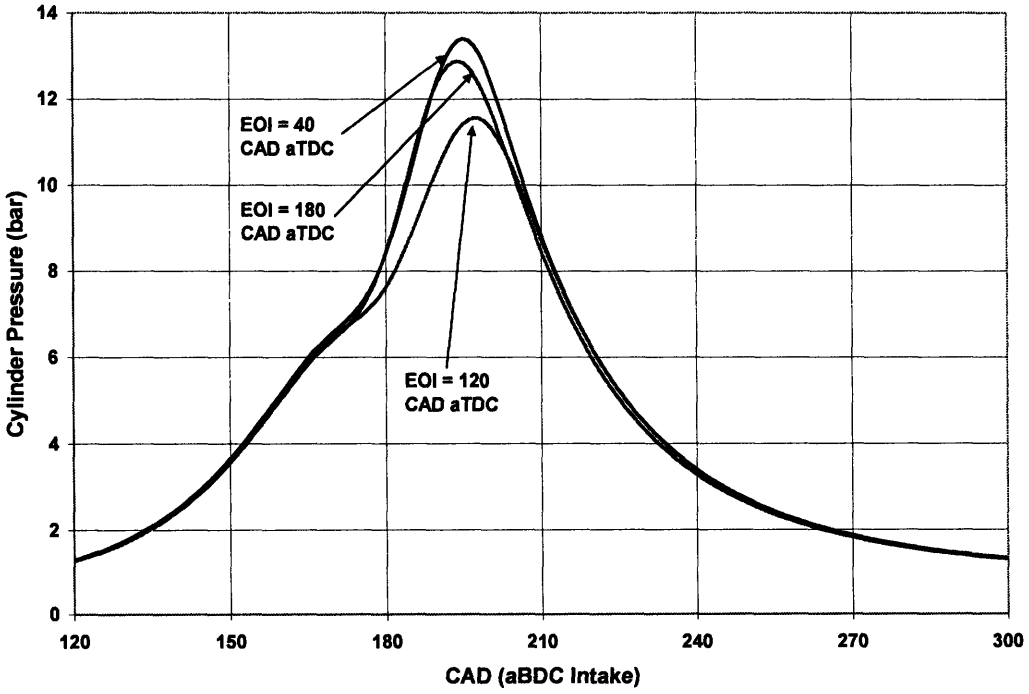

Figure 3-25: Cylinder Pressure for UTG 91 for coolant temperature of 80° C

3.6.2 85 % Ethanol and 15% UTG 91

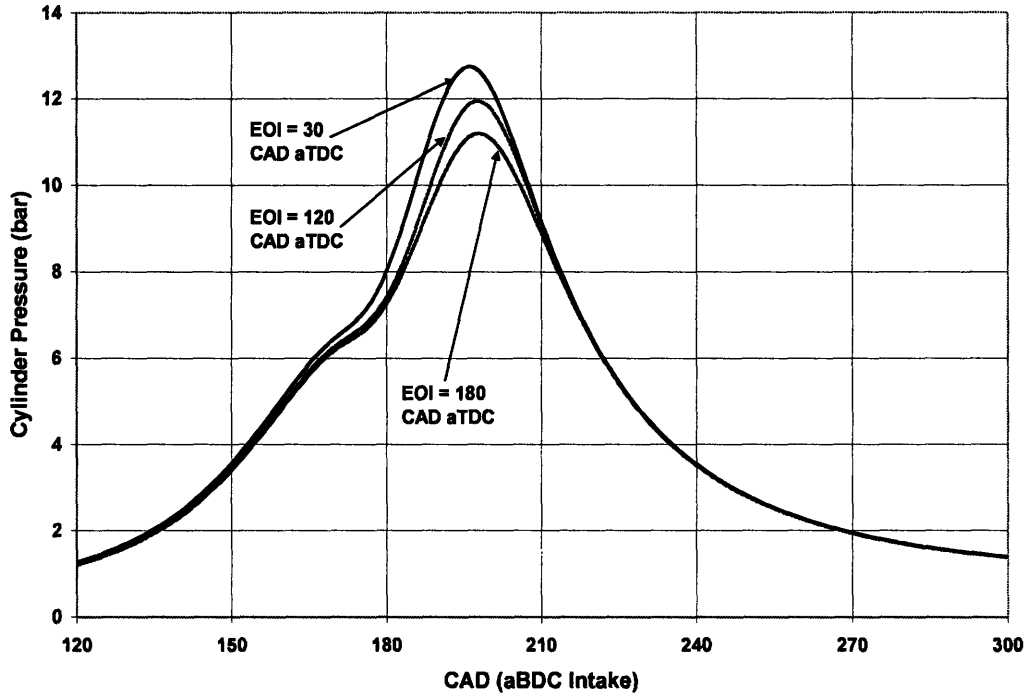

Figure 3-26: Cylinder Pressure for 85% ethanol and 15% UTG 91 for coolant temperature of 20° C

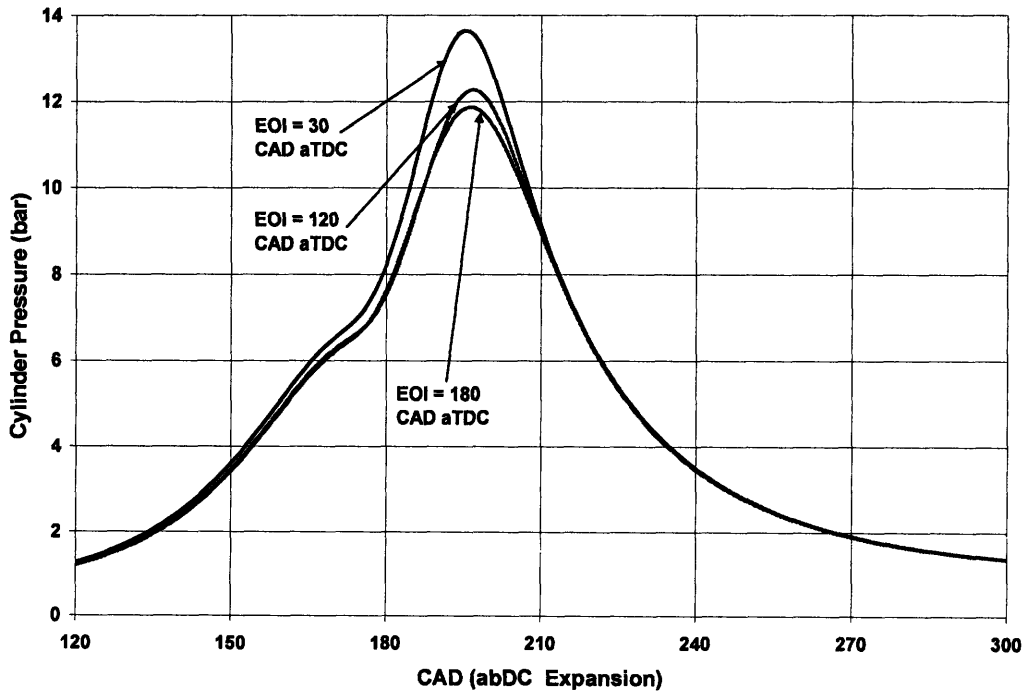

Figure 3-27: Cylinder Pressure for 85% ethanol and 15% UTG 91 for coolant temperature of 40° C

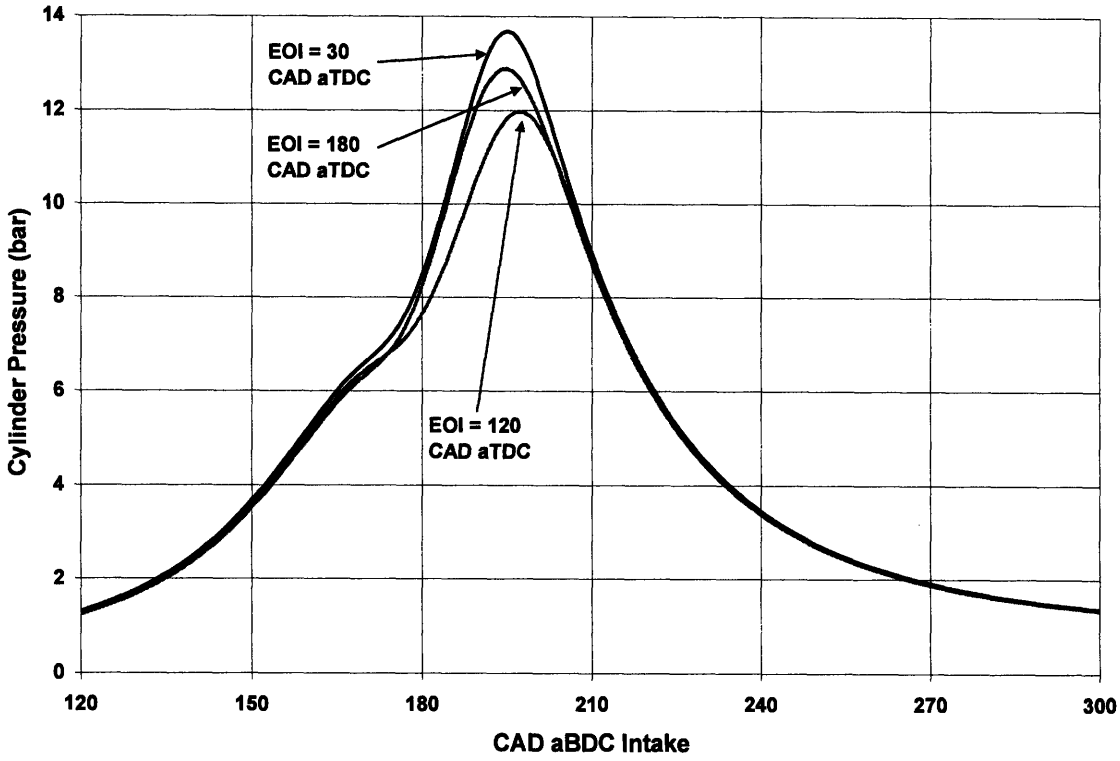

Figure 3-28: Cylinder Pressure for 85% ethanol and 15% UTG 91 for coolant temperature of 80° C

4 Summary

4.1 Conclusion

Experiments performed to evaluate the effect of engine temperature on hydrocarbon emissions showed a reduction in hydrocarbon emissions as a function of increasing temperature due to a reduction in the amount of mass in the crevices, lowered deposits, less saturation of fuel into the oil, and faster vaporization of the fuel. Experiments performed with an open CMCV showed a flattening of HC emissions between 40° and 70° C. It is not clear why this occurs, but it is possible that it is the result of inefficient mixing or liquid impingement. The hydrocarbon emissions of UTG 91 with the CMCV closed and isopentane with the CMCV open demonstrated a continuous reduction in hydrocarbon emissions as

temperature increased. The reduction in hydrocarbon emission was more dramatic for UTG 91, possibly because it is composed of several fuels each with its own boiling point.

The average hydrocarbon emissions as a function of injection timing demonstrated a similar trend for all fuels and temperatures. In every case, very early timing (~30 CAD aTDC Intake) resulted in high hydrocarbon emissions. These high emissions are most likely due to large levels of impingement on the cylinder walls and piston as well as poor initial mixing due to low intake velocities and the fuel charge being delivered into a low mass of air which is initially oversaturated. As injection timing is retarded the hydrocarbon emissions decrease due to an increase in charge velocity and mass and an increase in the clearance between the injector and piston.

The hydrocarbon emissions then begin to rise and peak at an EOI of approximately 150 CAD aTDC. The magnitude of this peak is fairly independent of temperature except for the 85% ethanol blend. As such it is likely a function of mixing and/or spray positioning for that injection timing. For the 85% ethanol blend at low temperatures, the continuous rise in emissions is likely due to ethanol having a high heat of vaporization which does not give the fuel enough time to vaporize at late injection timing with a 20° C coolant temperature which is well below the bubbling temperature of ethanol at a pressure of 0.27 bar.

The gross indicated fuel conversion efficiency data are more confusing. No standard explanation exists which can explain the trends. A possible hypothesis is for an EOI of 120 CAD aTDC, the fuel spray pattern and distribution is such that a large amount of fuel comes in contact with cooler portions of the cylinder wall and/or is unable to vaporize before being captured within the piston rings. Fuel blends containing high proportions of ethanol do not suffer from this problem as severely because ethanol almost entirely vaporizes once it reaches

its bubble point. However, if the engine is cold then substantial fuel loss occurs because the engine is not hot enough to vaporize the ethanol and thus a large portion of fuel is lost to the oil.

The plots of cylinder pressure as a function of crank position indicates that the lower efficiencies are associated with lower combustion pressure. Comparison of the pressure before combustion indicates a higher initial pressure for earlier injection timing for both fuels and the effect is more noticeable for the 85% ethanol blend. The difference may be because of an increase in heat transfer from the piston and cylinder walls.

Experimental measurement of the instantaneous hydrocarbon emissions near the exhaust valve have served to disprove the previous theory that the higher hydrocarbon emissions were due to a flow of liquid fuel into the exhaust valve. If such "short-circuiting" were to occur then a peak in hydrocarbon emissions would occur shortly after the opening of the exhaust valve because hydrocarbons would have accumulated within the vicinity of the exhaust valve and then be blown out of the cylinder.

4.2 Future Improvements

Several aspects of the experimental set-up can be improved for later experiments. One of the primary issues is the electrical set-up. The lab's electrical system is steadily being modernized and improved. However, electrical instabilities and ground shorts still exist which result in errors in the recording software. In addition, since the majority of the data acquisition system and instrumentation have been installed by students rather than licensed technicians there are several electrical problems. A primary example is that there is a -0.01 Volt drop between the measurement equipment and the National instruments chassis. Although this is not a large voltage loss, it still requires offsets to be added to all

measurements and adds additional sources of error to all measurements. A more dramatic problem is that the pressure reported by the MAP sensor varies depending of whether or not it is connected to the National Instruments chassis. Luckily, this error appears to disappear after running the system for 15 minutes; however, it clearly indicates that the instrumentation set-up should be reviewed and rewired to remove these problems.

Another aspect of the experimental set-up that should be addressed is the airflow meter. Analysis of the air flow meter data indicates that the values reported are incorrect. Pressure and vacuum testing of the hoses and seals has not revealed any leaks. However, it would be advisable to retest the system for any leaks using vacuum testing and pressurized tests with bubble solution on all seals. In addition, the airflow meter should be sent back to the manufacturer for recalibration since the certification time has expired and the meter readout indicates this fact.

Another aspect of the experimental set-up that it is key to be aware of is the pressure transducer for measuring in-cylinder pressure. Although the pressure transducer has been placed in such a way as to minimize the thermal shocks it is exposed to, it can still become broken and malfunction in a way that is not obvious. As such, it is critical for anyone performing tests to sporadically analyze the pressure traces for any anomalies which might be indicative of sensor malfunction.

Discussion has also occurred about changing the injectors used in the engine. The current injectors are not a well supported type and it has proven near impossible to find replacement parts. In addition, the injectors are not designed to be used with ethanol blend fuels. This issue has been partly addressed by replacing all the o-rings with an ethanol

resistant polymer. However, it is not clear if the internal seals and functional components of the injector will be able to withstand prolonged testing with fuels containing ethanol.

Currently, new injectors have been purchased; however, the changing of the injectors will introduce a new variable into the testing and will likely require the redoing of previous tests in order to provide comparable data. Moreover, the new injectors are not designed to work with the current fuel rail. A new fuel rail will have to be purchased or acquired from GM and modified to work in the current set-up.

4.3 Future Experiments

A list of potential future experiments and tests is shown below in order of relative importance.

1. A primary problem is attempting to explain the behavior of the fuels at different temperatures is a lack of knowledge of in cylinder temperatures of the air-fuel mixture prior to combustion and more importantly the temperature of the piston and cylinder walls. Modifying the engine for thermocouples inside the cylinder would require significant modification of the engine. However, if such data could be obtained then it would be incredibly valuable for determining how much charge cooling occurs and for predicting how much fuel vaporization has occurred and will occur. Measurement of piston and cylinder wall temperature would be even more difficult. However, it may be possible to ask the corporate sponsors to run CFD codes to predict the temperature distribution. Such information would be incredibly valuable in determining if fuel loss is occurring due to contact with cold surfaces inside the engine.

2. Determination of the actual spray pattern for the injector and where the fuel is likely to impinge on the piston and cylinder walls would provide insights into the causes for

trends in engine efficiency and hydrocarbon emissions. As of yet we have no knowledge of the actual spray pattern for the injectors in the engine. Images of spray patterns exist for similar injectors; however, it would be better to have the spray pattern for the particular injector in our engine. A possible solution that has been suggested is to remove the spark plug and place a borescope into the engine which can then be used to observe the spray pattern of the injector. This has the additional advantage of showing where the fuel impinges on the piston and cylinder walls. The best possible solution would be if the borescope could be inserted and sealed so as to allow the engine to run without firing. This would allow the spray distribution during actual engine operation to be seen. Issues such as providing sufficient light, adjusting the fuel control system for a single firing, and preventing damage to the borescope would have be addressed for these experiments to be performed. However, the benefits would be immense if it could be done.

3. The current system for filling the accumulators has been designed to build upon the previous system as much as possible. As a result, the fuel pump and fuel filter set-up has not been changed. Since all fuels pass through the same fuel filter, fuel contamination occurs. Among the ethanol blends and gasoline, the effect of the contamination is likely minimal. However, in the future if pure chemicals are to be tested, such as isopentane and ethanol, it would be better if a different fuel filter could be used. In addition, it would also be beneficial if the "loop" line could be adjusted so that it has the potential to return the fuel to a waste fuel container rather than container from which it is drawing fuel. This would greatly reduce the complexity of changing

over from filling an ethanol blend accumulator to filling the gasoline accumulator and would result in more thorough and efficient flushing of the fuel lines.

4. Currently the actual level of HC emissions for ethanol blend tests cannot be measured because the FFID is not as sensitive to oxygenated compounds. As such, it would be good to collect exhaust gas samples from the mixing tank and send them for mass spectroscopy as per the literature procedure. Mass spectroscopy cannot be used to measure the instantaneous HC emissions, but would allow the average HC emissions in the exhaust mixing tank to me accurately measured.

5. Another improvement would be to measure the instantaneous CO emissions near the exhaust port. The average HC emissions in the mixing tank are not high enough to make any clear determinations about the level of mixing that is occurring. Since post-stream oxygenation of CO into CO_2 reduces the levels of CO, measuring closer to the exhaust valve would provide more useful data. In addition, with the current set-up the exhaust gas must mass through the condenser, reach a steady state level within the liquid trap, and then pass into the emissions analyzer. This provides additional time for oxygenation to occur and also increases the time between tests. The lab has a fast CO & CO_2 analyzer and the exhaust manifold has already been equipped with a fitting for inserting sampling probes. The additional data might require a modification to the data acquisition software since for the required sampling rate, the system has reached its maximum number of input channels.

References

1. Cheng W.K., Hamrin D., Heywood J.B., Hochgreb S., Min K., and Norris M., "An Overview of Hydrocarbon Emissions Mechanisms in Spark-Ignited Engines." SAE Paper 932708, 1993.

2. Zhao, F., Harrington, D.L., Lai, M., Automotive Gasoline Direct-Injection Engines, Society of Automotive Engineers, Inc., Warrendale, PA, 2002.

3. Andreisse, D., et al., "Assessment of stoichiometric GDI engine technology," Proceedings of AVL Engine and Environment Conference, 1997.

4. Anderson, R. W., Yang, J., Brehob, D.D., Vallance, J.K., Whiteaker, R.M., "Understanding the thermodynamics of direct-injection spark ignition (DISI) combustion systems: an analytical and experimental investigation," SAE Paper 962018, 1996.

5. Harada, J. Tomita, T., Mizuno H., Mashiki, Z., Ito, Y., "Development of direct-injection gasoline engines," SAE Paper 970540, 1997.

6. Tomoda, T. Sasaki, S. Sawada, D., Saito, A., Sami, H., "Development of direct-injection gasoline engine – study of stratified mixture formation," SAE Paper 970539, 1997.

7. Heywood, John. Internal Combustion Engine Fundamentals. New York: Mc-Graw Hill Book Company, 1988.

8. Radovanovic, M., "Assessing the Hydrocarbon Emissions in a Homogenous Direct Injection Spark Ignited Engine," MIT M.S. Thesis, August 2006.

9. GM/Fiat Paper. Internationales Weiner Enginesymposium, 2003.

10. International Occupational Safety and Health Information Centre (CIS). March 2008. http://www.ilo.org/public/english/protection/safework/cis/products/icsc /dtasht/index.htm

11. Product information sheet: XEM4CX631-85A Winter. Haltermann Products.

Appendices

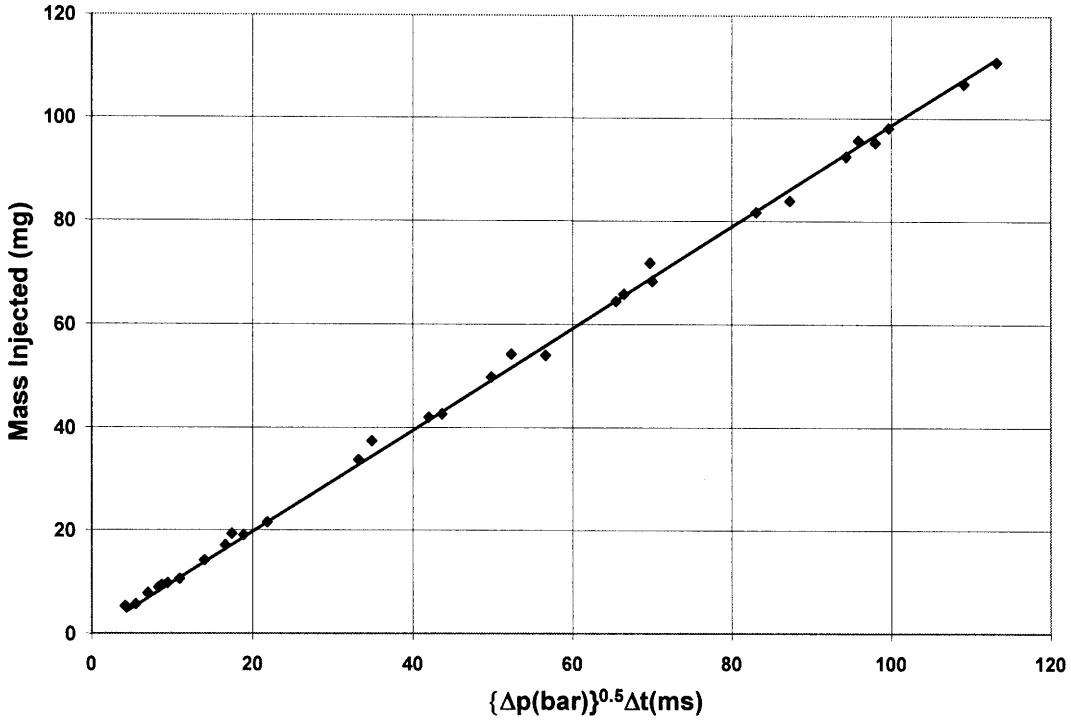

Appendices 1: Injector Calibration Curve for UTG 91

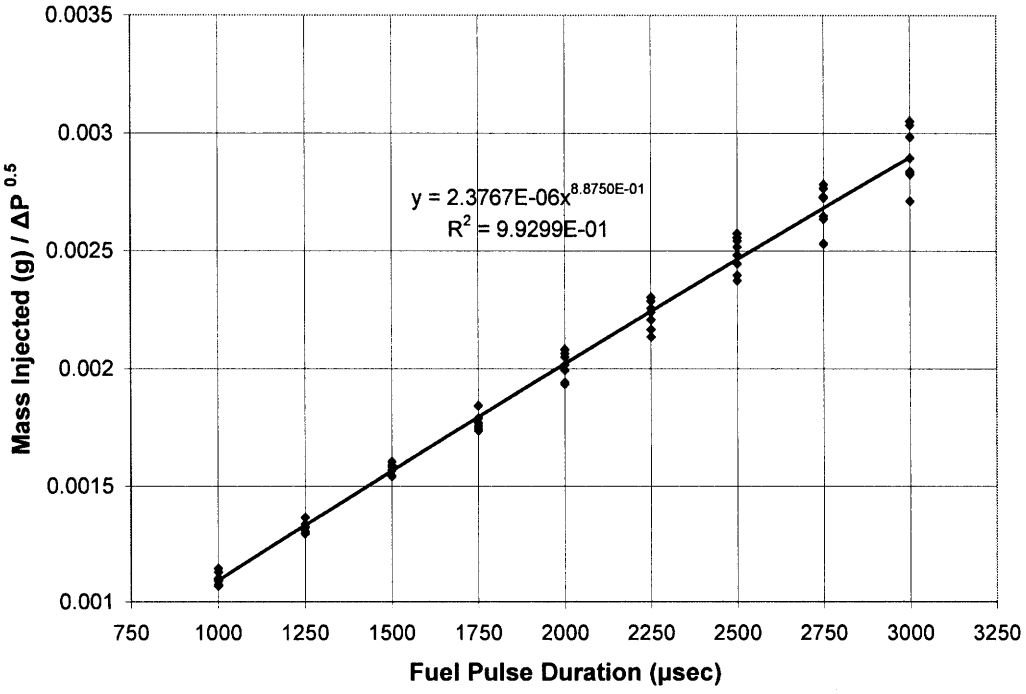

Appendices 2: Injector Calibration Curve for 15% ethanol by mass blend

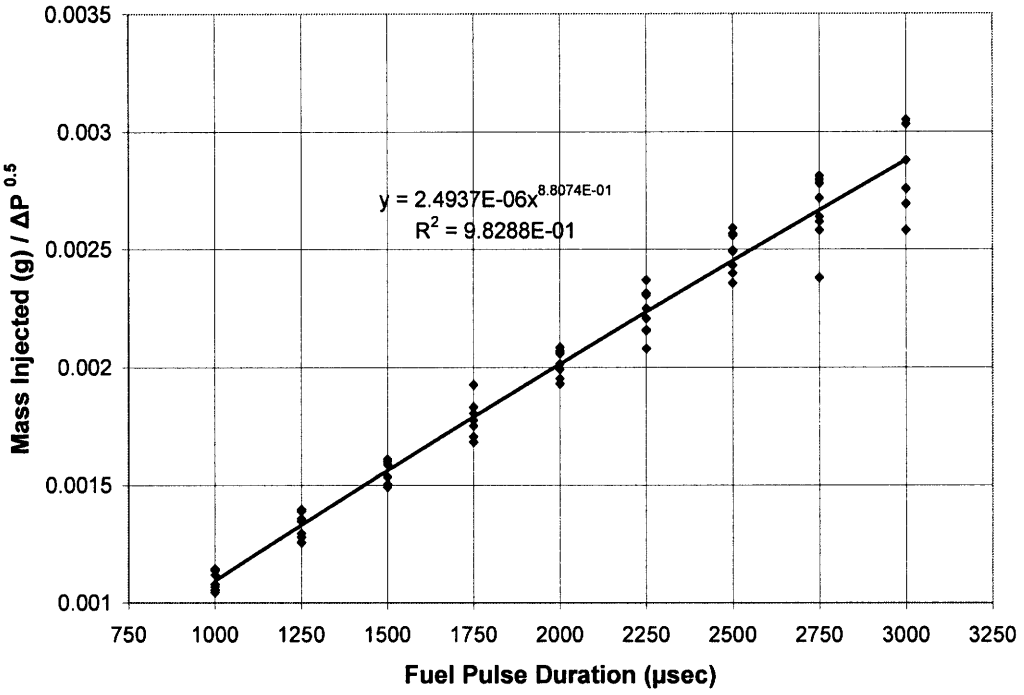

Appendices 3: Injector Calibration Curve for 40% ethanol by mass blend

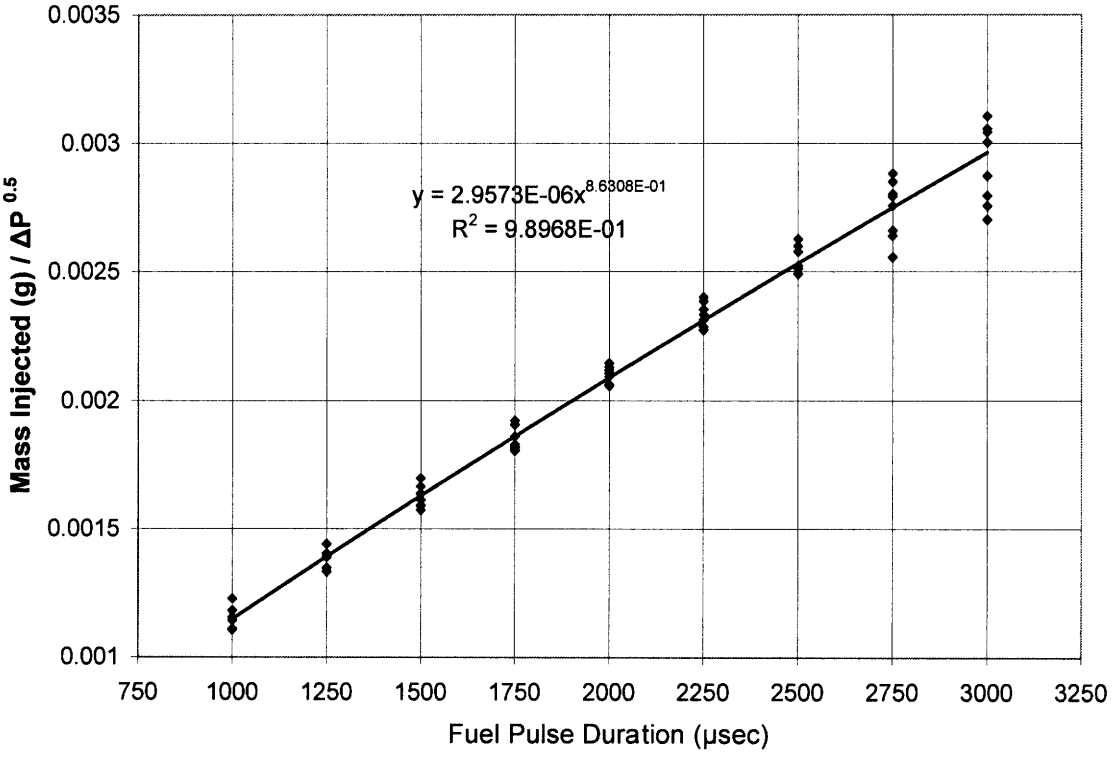

Appendices 4: Injector Calibration Curve for 85% ethanol by mass blend

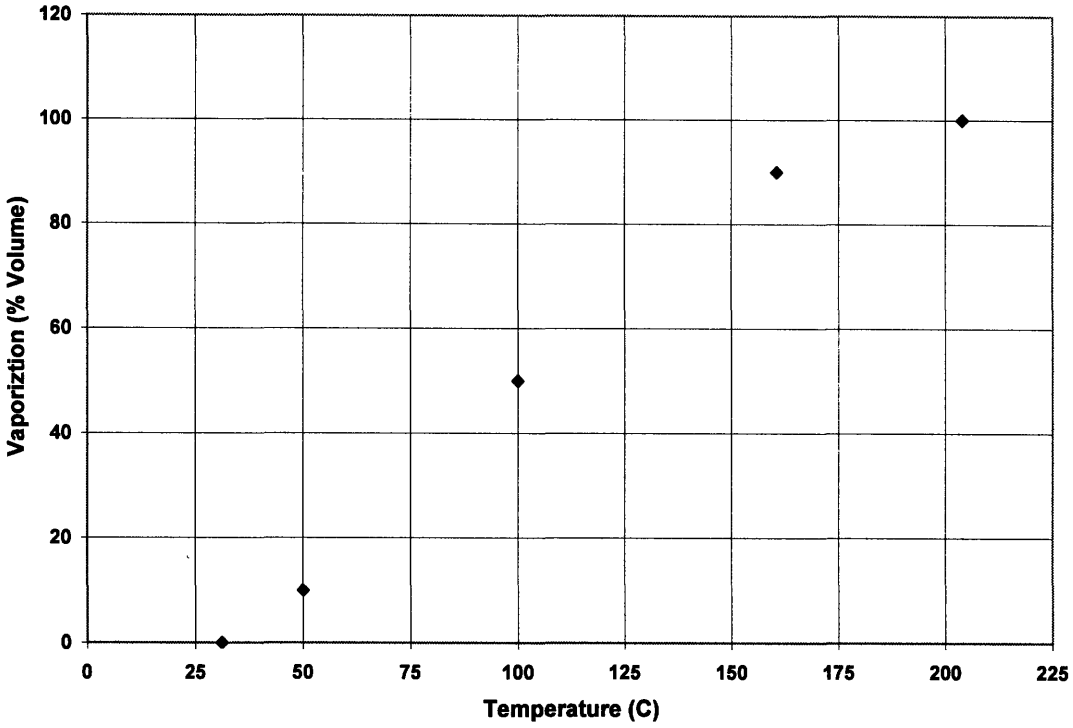

Appendices 5: Distillation curve for UTG 91

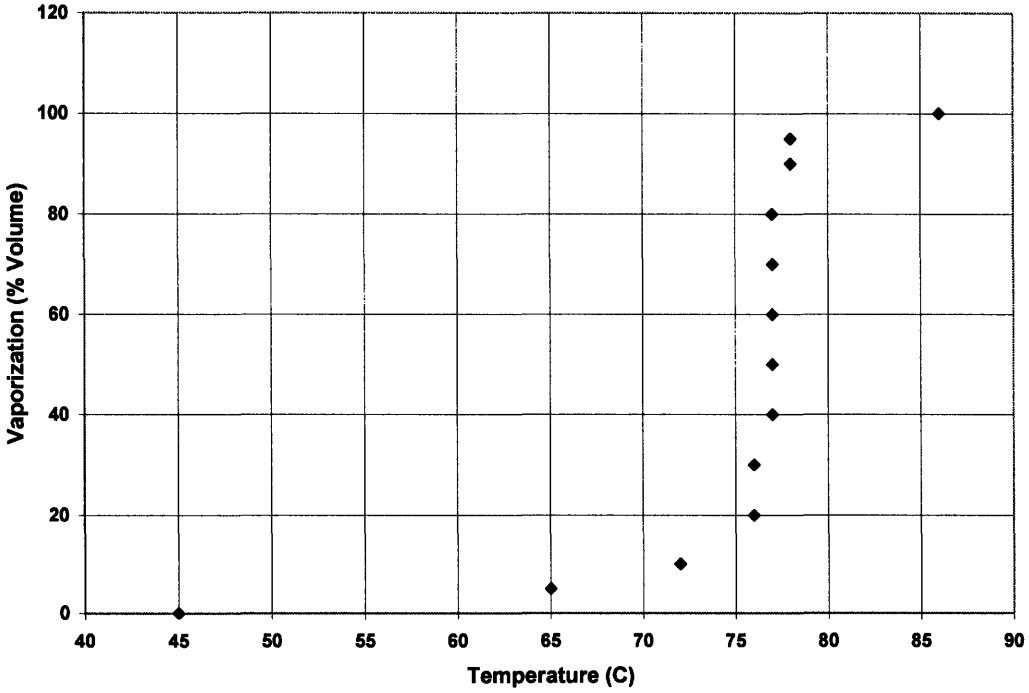

Appendices 6: Distillation curve for a commercial E85 blend [11]

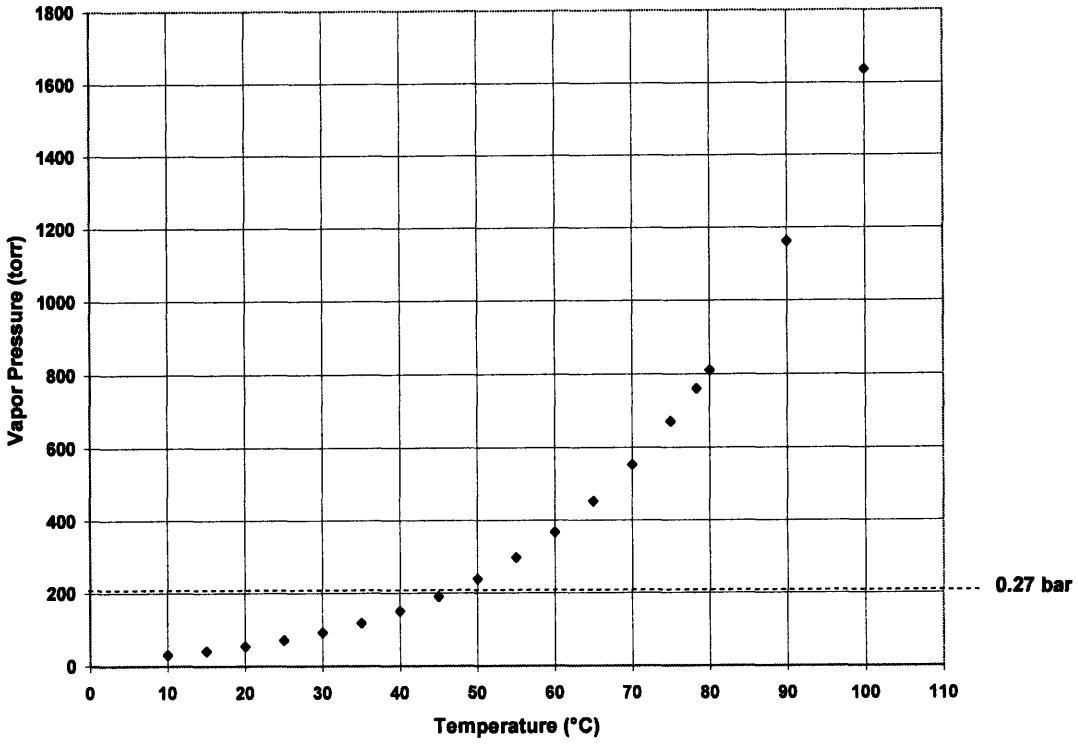

Appendices 7: Vapor pressure curve for pure ethanol as well as MAP condition used for testing

Property	Typical Value	Specification	Test Method
Specific Gravity at 60/60 °F	0.7350	0.7343 – 0.7440	ASTM D 4052
API Gravity	61.0	Report	ASTM D 1250
Copper Corrosion, 3 h at 50 °C	1	1 max	ASTM D 130
Existent Gum (washed), mg/100 mL	2	5 max	ASTM D 381
Sulfur, ppm	130	1000 max	ASTM D 5453
Reid Vapor Pressure, psia	9.0	8.8 – 9.2	ASTM D 5191
Lead, g/gal	0.0010	0.0050 max	ICP/OES
Phosphorus, g/gal	0.001	0.002 max	ICP/OES
Hydrogen, wt %	13.7	Report	ASTM D 5291
Carbon, wt %	86.3	Report	ASTM D 5291
Carbon Density, g/gal		Report	Calculated
Distillation Range at 760 mmHg, °F			ASTM D 86
Initial Boiling Point	88	75 – 95	
10%	122	120 – 135	
50%	212	200 – 230	
90%	321	300 – 325	
End Point	399	415 max	
Oxidation Stability, min	> 1440	1440 min	ASTM D 525
Heat of Combustion, Net, Btu/lb	18500	Report	ASTM D 240
Composition, vol %			ASTM D 1319
Aromatics	24.0	35.0 max	
Olefins	6.0	10.0 max	
Saturates	70.0	Report	
Research Octane Number	90.6	90.3 – 91.7	ASTM D 2699
Motor Octane Number	82.6	Report	ASTM D 2700
Anti-Knock Index, (R+M)/2	86.6	87.0 max	Calculated
Sensitivity	7.8	7.5 min	Calculated
Oxygenates, vol %		0.0 max	Chromatography
Benzene, vol %		Report	Chromatography

Appendices 8: Properties of UTG 91